Theses, Dissertations and Culminating Projects

5-2019

Elemental Analysis of Species Specific Wood Ash : A Pyrogenic Factor in Soil Formation and Forest Succession for a Mixed Hardwood Forest of Northern New Jersey

Michael T. Flood
Montclair State University

ABSTRACT

Fire is a significant environmental perturbation to forests where vegetation transforms from biomass to ash, potentially releasing stored chemical elements to soils. While much research acknowledges variation in ash composition among different vegetation types (grasses, trees, shrubs and vines), less has focused on interspecific variation among trees and the elemental influx soils receive. Therefore, this research sets out to: (1) identify major, trace, and rare earth element (REE) concentrations by inductively coupled plasma mass spectroscopy (ICP-MS) in ash derived from fifteen tree species, (2) determine likely elemental enrichment to post-fire soils, and (3) assess variability in ash chemistry and color among different tree species. Traditional color assessments classify ash on a grey scale, but ash samples in this study had distinct color hues and coalesced in two groups. A significant negative correlation existed between SiO_2 and CaO among all ash samples. Ash samples were more concentrated in MnO, MgO, CaO, K_2O, P_2O_5, Ni, Cu, Zn, Sr and Ba than soil, as well as in all REE's (La through Lu). Ash from *Populus grandidentata, Betula lenta,* and *B. alleghaniensis* had greatest enrichment in Zn and Ba while ash from *Fraxinus americana* had elevated Cu and Sr. This clearly shows significant chemical variability in ash, possibly derived from preferential element uptake by certain tree species to satisfy physiologic and metabolic nutrient requirements. All REE's were 10-15 times greater in ash than soils. Little preferential uptake of any one REE exists as trees might passively sequester all these elements together, bound to essential nutrients. This research provides an important understanding of the complexities surrounding fire's impact on biogeochemical cycling.

Key Words: Wood Ash, Biogeochemical Cycling, Forest Fires, Soils, Trace Elements

MONTCLAIR STATE UNIVERSITY

Elemental Analysis of Species Specific Wood Ash: A Pyrogenic Factor in Soil Formation
and Forest Succession for a Mixed Hardwood Forest of Northern New Jersey

By

Michael T. Flood

A Master's Thesis Submitted to the Faculty of

Montclair State University

In Partial Fulfillment of the Requirements

For the Degree of

Masters of Science

May 2019

School: <u>College of Science and Mathematics</u>

Department: <u>Earth and Environmental Studies</u>

Thesis Committee:

Dr. Gregory Pope
Thesis Sponsor
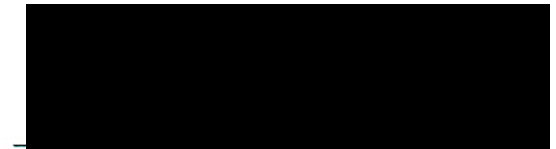
Dr. Jennifer Callanan
Committee Member
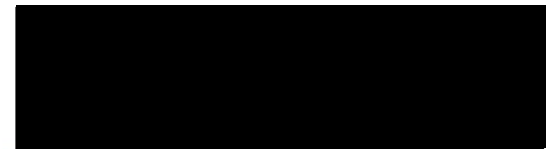
Dr. Joshua Galster
Committee Member

ELEMENTAL ANALYSIS OF SPECIES SPECIFIC WOOD ASH: A PYROGENIC
FACTOR IN SOIL FORMATION AND FOREST SUCCESSION FOR A MIXED
HARDWOOD FOREST OF NORTHERN NEW JERSEY

A THESIS

Submitted in partial fulfillment of the requirements

For the degree of Master of Science

By

Michael T. Flood

Montclair State University
Montclair, NJ
2019

ACKNOWLEDGEMENTS

plants. All of these viewpoints were integral in data assessment and provided many

mechanisms to explain various geochemical results/trends. Thanks to Kelly Zimmerman

and Diane Hagmann for reviewing certain section of this manuscript and providing

commentary on the writing.

Finally, I would like to thank my family for support and good laughs throughout

the thesis process. I dedicate this thesis to my grandparents, all of whom taught me the

values of hard work, devotedness to one's aspirations, and to always have an open mind

about learning new things.

TABLE OF CONTENTS

LIST OF FIGURES

LIST OF TABLES

1. INTRODUCTION

As uncontrolled forest fires consume thousands of acres and inflict upwards of $70 billion (in 2016 $) annually across the United States (Thomas *et al.,* 2017), this environmental perturbation not only poses a significant hazard to human welfare but also provides critical ecological impacts (Flannigan *et al*., 2000; Certini 2005). Fuel load (amount of combustible material), burn duration, and soil moisture dictate potential fire severity, while maximum burn temperature dictates the degree of impact to forested ecosystems and soils (Verma & Jayakumar, 2012; Bodí *et al*., 2014). As shown in Figure 1.1, burn temperature is a key control over physical and chemical processes in soils exposed to fire. Whether uncontrolled or controlled, fire results in the sudden conversion of living material (biomass), dead material (necromass), and soil organic matter (SOM) to mineral ash and/or charred material.

Upon burning, mineral ash has different physical and chemical properties from its parent material (Bodí *et al.*, 2014) and provides inorganic major, trace, and rare earth elements (REE's) to forest soils (Pope *et al.,* 2012; Darley, 2017). The variance in elemental composition among species specific wood ash is, however, less certain (Ågren & Weih, 2012). Ash composition is likely influenced by vegetation since some vegetation species have a greater affinity to uptake certain elements (e.g., calcium, zinc, manganese, cadmium, and chromium) over others (Thomas, 1969; St. Clair & Lynch, 2005; Bodí *et al.,* 2011; Petrova *et al.*, 2014). This means ash chemistry likely varies based on species burned. Research acknowledges this variation in ash chemistry among different vegetation types (grasses, trees, shrubs and vines) (Bodí *et al*., 2014), but less has focused on interspecific ash variation among trees. Therefore, this research helps to better answer

questions previously proposed by Pope *et al.* (2012), Callanan *et al.* (2017) and Darley (2017) in work relating ash chemistry, soil signatures, and vegetative species to post-fire biogeochemical cycling in soils.

1.1 Forest Fire Concerns for the Eastern US

Much fire research focuses on semi-arid forests with frequent forests fires (e.g., the western US and boreal Canada). However, less is known about fires within temperate forests where decades of fire suppression policy and increased tree mortality have contributed to high fuel loads (Kodas, 2012). Coupled with warming conditions --where dry areas are likely to become drier, wet areas wetter, and greater variation in climate extremes -- fire hazards are likely to increase (Westerling *et al.,* 2006). The culmination of these factors, plus high population density surrounding temperate forests, will increase fire risk (Flannigan *et al.,* 2000).

A prominent concern to forest managers is finding a balance between fire frequency and fuel reserves (Stephens & Ruth, 2005; Hutto *et al*., 2016). Even with much time and financial resources spent on fire suppression activities, the annual acres consumed by wildfires across the US increased over the past several decades (Stephens & Ruth, 2005). For nearly a century, the main federal forest fire policy focused on fire suppression (Stephens & Ruth, 2005). This suppression neglected the ecological benefits of forest recovery and forest resiliency brought about by fire (Hutto *et al.*, 2016). Combustible fuels have been allowed to accumulate which has led to changes in fire behavior (Westerling *et al.*, 2006). Typical low intensity, small fires, consumed floor and lower story vegetation, but the accumulation of burnable fuels has allowed for larger, more severe, fire events. Small fire outbreaks can quickly become "monster" fires, ravishing

2

large tracts of land, removing high amounts of soil organic matter, and burning at higher temperatures when extreme drought conditions persist (Hutto *et al,*. 2016).

Although less susceptible, concerns still exists about how forest fire regimes in eastern US forests will change as climate variability, fire suppressive activities, and tree mortality can increase fire occurrence. These factors can potentially lead to higher quantities of "burnable" fuels and greater forest fire risk. When material accumulation rates exceeds decomposition rates, fire occurrences are more likely. Flannigan *et al.* (2000) expects a likely increase in the annual amount of burned area across US, with greater frequency and intensity of fires due to dryer, more flammable, conditions. For New Jersey, temperatures have been and will warm. Since the 1970's average temperatures have increased by 0.65 to 0.70 °C per decade, with the greatest warming occurring during the winter months (Evans & Perschel, 2009). By 2030 temperatures are expected to increase by 1 °C over the 1960-1990 average and by 3.2 °C in 2100 (Evans & Perschel, 2009). With this in mind, the NJ Department of Environmental Protection, Forest Fire Service (2014) mapped fuel load hazards and associated fire risks for the state (figure 1.2). Forests along the northeast-southwest traversing Kittatinny Ridge of northwest NJ and the Pine Barrens of southern NJ have elevated fuel loads (figure 1.2a).

Recent tree mortality caused by biological agents and storm damage continue to elevate fuel reserves (Hicke *et al.,* 2016). Many tree species within New Jersey are in decline from a variety of insect species. A well-known insect defoliator of oak trees is the gypsy moth (*Lymantria dispar dispar*). Accidently introduced to the US in 1869, this insect killed or weakened many oak species in New Jersey since 1970 (Collins and Anderson, 1994). Other insects threatening northeastern forests include those listed in

table 1.1, along with genera of trees in decline due to insect infestation. Disease vectors (viruses, bacteria, and fungi) also pose a potential threat to certain tree species. Dutch elm disease targets elm trees (*Ulmus spp.*), beech bark disease attacks beech trees (*Fagus* spp.), black knot (*Dryopteris morbosum*) slowly kills trees in the *Prunus* genera (plum and cherry trees), and oak wilt (caused by the *Ceratocystis fagacearum* fungus) leads to further declines in oak species (*Quercus* spp.) (Foster & Orwig, 2006). Under warming conditions many of these insects and diseases are likely to expand current ranges and become more problematic (Evans & Perschel, 2009). More frequent, higher intensity storms (e.g., hurricanes and ice storms) will cause damage to tree stands, further contributing to species mortality and combustible fuel loads (Kodas, 2012).

Human population density indirectly complicates these issues further. The eastern US is more densely populated than the west, meaning any major fire outbreak in the east will likely inflict more costs than similar magnitude fires in the western US (Radeloff *et al.,* 2005). Radeloff *et al.* (2005) found that across the continental US one tenth of the area and one third of homes are situated in Wildland-Urban Interfaces (WUI). A higher proportion of homes in the WUI were located in the eastern US. These authors delineated WUI as "areas where structures will likely be destroyed by wild fires when fuel and weather conditions are conducive for fire outbreaks". This alarming statistic, compounded by a greater potential for future forest fires in the northeast, warrants a rethinking of forestry management with the use of controlled burns to reduce fuel loads, speed up biogeochemical cycling in forest, and bolster forest health (Hutto *et al.,* 2016).

1.2 Pyroecology of Forests

Fire impact to forests is much like an herbivore: consuming organic molecules and converting them to byproducts (Bond & Keeley, 2005). However, the mineral ash and heat byproduct of fire differentiates this disturbance from typical herbivory. Fire has the capacity to increase soil fertility, intensify weathering processes, stimulate regrowth of vegetation, and enable secondary forest succession (Santin & Doerr, 2016). Such ecological benefits are dependent on fire frequency and flammability of the ecosystems, along with the amount of biogeochemical flux during pyrogenic disturbances.

1.2.1 Frequency and Flammability: Areas frequented by fire (i.e., once or twice a decade) are dominated by woody plant species of shortened stature, thick insulated bark, swollen underground roots, self-pruning of lower dead branches and seeds encapsulated by a thick protective coating (Bond & Keeley, 2005; Keeley *et al.,* 2011). These plant characteristics are typically present in mid-latitude forests with frequent ground fire regimes (Keeley *et al.,* 2011). Self-pruning ensures a gap between accumulated fuel sources on the ground and living branches in the crown during a ground fire outbreak (Keeley *et al.,* 2011). Where crown fires predominate, species have adapted traits to *enhance* flammability in order to release seeds and reproduce. Some of these traits include: having small leaves, thin bark, elevated concentrations of volatile organic compounds, serotinous cones and the ability to retain dead branches (Keeley *et al.,* 2011). Dead branch retention, as seen with many high latitude pines species (*Pinus sp.*), enables fire to "creep" into the tree canopy and release seeds trapped in serotinous cones (Bond & Keeley, 2005; Keeley *et al.,* 2011). Serotinous cones have a thick coating of volatile organic resins which must be melted off before the cone can open (Keeley *et al.,* 2011).

Therefore, not only climatic conditions, but dominant tree species can influence the potential for a forest to burn (Bodí *et al.,* 2014).

1.2.2 Forest Diversity. Fire frequency influences species diversity and the overall forest mosaic. Whether fires are frequent (one to two times a decade) or infrequent (once every 50 to 100 years), forests with uninhibited fire regimes often have greater species diversity than forests under fire suppression (Cohn *et al.,* 2015). Regular fire occurrence creates a network of "fire patches" within a contiguous forest, where different patches are at different successional stages (Cohn *et al.,* 2015). Figure 1.3 highlights the process of secondary forest succession under ideal conditions for a specific burned patch. Initially fire removes most of the underlying vegetation and creates a gap in the overriding tree canopy. Within these gaps, species can colonize, through various dispersal mechanisms, and remain younger in age than the surrounding forest for some time (Cohn *et al.,* 2015). Over large spatial-temporal scales, recurrence of fire creates a contiguous forest of uneven-aged patch bodies.

Current timber production tries to mimic fire induced forest patches by clear cutting certain areas of forest, but the ash component remains missing. Without ash, soil nutrients are not replenished quickley, which slows the rates of revegetation and forest succession. As Pereira *et al.* (2012) noted, ash is a key source of nutrients for forest recovery post-fire. Thiffault *et al.* (2008) noted higher concentrations of nitrogen rich aromatic organic compounds, calcium, and magnesium in soils at wildfire sites as opposed to clear cut sites. Pitman (2006) argued a single application of wood ash per tree stand rotation (the time from planting to harvesting) would replace all the necessary nutrients needed for tree regrowth, except for nitrogen.

1.2.3 Impacts of Anthropogenic Fire Suppression. Every forest has a unique fire recurrence interval, but humans have altered fire recurrence by promoting fire suppressive policies. Such policies have nearly eliminated fire disturbance from many US forests, heightening current fire risk and resulting in many ecological problems (Stephens & Ruth, 2005). As addressed by Arthur *et al.,* (2015), loss of large scale forest disturbances in Appalachian hardwood forests have homogenized forest structure and reduced canopy openness. These forests have lost many early successional, light dependent species, favoring a shift towards shade-tolerant, late successional species (Figure 1.3). Some species, like oaks (*Quercus sp.*) and hickories (*Carya sp.*), are disturbance dependent for growth and can re-sprout after fire damage as long as the root base is left undisturbed (Collins & Anderson, 1994). Other species, such as maples (*Acer sp.*), cherries (*Prunus spp.*), and birch (*Betula* spp.), tend to have a lower capacity to regrow after fire damage (M. Hazen, personal communication). Lack of fire disturbance in Appalachian hardwood forests resulted in a shift from mid-successional oak dominance, to late successional maple (*Acer spp.*) and black gum (*Nyssa sylvatica*) dominance (Arthur *et al.,* 2015). Subsequently, Arthur *et al.* (2015) showed prescribed burns having some ability to curb the expansion of maple dominance, especially when prolific stump sprouting of resilient hardwood species (*Quercus spp.* and *Carya spp.*) occurred. Similarly, prescribed burns in the Delaware State Forest of Pennsylvania have targeted the propagation of *Quercus spp*. for timber production by removing *Betula spp.* and enriching soil nutrients with the fire ash (M. Hazen, personal communication).

Studying savannah ecosystems, Bond and Keeley (2005) indicated fire suppression as a key contributor to decreased species diversity. In some areas studied, these ecosystems

have lost as much as 50% of the native plant species. Fire suppression over a long time can lead to biome switches because species once incapable of surviving under frequent fire regimes now have a chance to colonize (and out-compete) the fire adapted species. This was seen as a switch from grasslands to forest ecosystems (Bond & Keely, 2005). Some forests have now gone "un-burned" for over a hundred years which has caused shifts in ecosystem structure and functions, especially in the understory. Increases in canopy tree density have created a shadier understory, meaning a loss of light dependent understory growth (Bond & Keely, 2005; Arthur *et al.* 2015).

1.3 Fire and Soils

Fire has an important ability to shape forest structure, and with it, soil development. Direct effects of fires on soil properties focuses on heating and fluxes of organic and mineral materials (Santin & Doerr, 2016). Many authors have suggested fire as the seventh soil forming factor (additional to: climate, organisms, relief, parent material, topography, and time) with a profound disturbance on soil formation and weathering processes (DeBano, 2000; Verma & Jayakumar, 2012; Certini, 2013). Fire's influence over soil properties is regulated by how long the fire occurred (duration) and the temperature of the fire (intensity) (Certini, 2013). Other factors such as prior weather conditions, soil moisture, landscape geomorphology, type of fuel, amount of fuel, and time of year also influence fire dynamics (Peteira *et al.,* 2012).

Changes in soil properties, such as soil organic matter, hydrophobicity, texture, structure, and iron oxidation (color) are key fire signatures used to judge fire severity (Certini, 2013). However, the amount of soil moisture present at the time of burning determines the total impact on the soils (Certini, 2005; Bodí *et al.,* 2014). Initially,

temperature increases are limited to the upper 5 centimeters of the soil profile and the degree of warming is regulated to 95°C by water's latent heat of vaporization (Certini, 2013). When all non-molecular soil moisture vaporizes, soil temperatures can reach 200 - 300°C and temperatures increase deeper within the soil profile (Debano *et al.,* 1998; Certini, 2005). A thermal gradient forms where temperatures can rise above 150°C in the first 5 cm but little temperature increases beyond 30 cm depth (DeBano, 2000). In oxygen abundant conditions, fire temperatures can reach 450-1400°C with a mixture of charred mineral ash remaining. When oxygen is limited (smoldering conditions) temperatures reach 250-450 °C and result in more complete combustion of organic material (Bodí *et al*, 2014).

1.3.1 Soil Organic Matter (SOM). Ground fires cause organic matter combustion at the surface horizons (O and A), but the extent of combustion is dependent on fire intensity, soil moisture content, and type of vegetation burned (Verma & Jayakumar, 2012). Low temperature fires (less than 300°C) leave most of the soil carbon in the soil. Alternately, high temperature fires (over 500°C) burn the soil organic matter and convert it to mineral ash. Transferring organic compounds to mineral compounds rapidly supplies the soil with necessary nutrients for landscape recovery (Pereira *et al.,* 2012).

1.3.2 Color: Soil reddening occurs as iron undergoes thermal alterations. For this phenomenon to occur, fire temperatures need to exceed 600°C for over 45 minutes (Verma & Jayakumar, 2012; Certini, 2013). Due to heterogeneity of fire intensity within a fire event, soil reddening is poorly distributed and becomes a local indicator of extreme fire conditions (Verma & Jayakumar, 2012). Smith *et al.* (2017) found reddened soils in burned areas of the Cascade Mountains had reduced nutrient concentrations. The lower

nutrient concentrations persisted for multiple years after the fire event. Nutrient loss by scorching soils potentially poses significant limitations to soil-redevelopment and productivity (Smith *et al.,* 2017).

1.3.3 Texture. Under high burn temperatures (over 500 °C), Ulery *et al.* (1996) and Reynard-Callanan *et al.* (2010) noted decomposition of phyllosilicate clays within the top few centemeters of the soil-fire interface. Clay decomposition remained noticeable for the next three years along with increases in soil bulk density (Ulery *et al.,* 1996). Collapsed clay minerals and ash accumulation likely reduces void space by "clogging" soil pores (Certini, 2005). Additionally, very coarse grained components (cobbles and boulders) can undergo thermal dilation (Blackwelder, 1933; Certini, 2013; Schaetzl & Thompson, 2015). Rapid temperature changes cause expansion and contraction, which exploits weaknesses with in the rocks and fractures them into smaller components (Blackwelder, 1933; Schaetzl & Thompson, 2015).

1.3.4 Nutrient Availability. One of the most important aspects of fire on soil properties is the influx of nutrients and elements from ash (Pitman, 2006; Augusto *et al.* 2007; Darley, 2017). As biomass undergoes combustion, once bound elements are released into the environment via volatilization to the atmosphere, deposition to the soil as ash, or sequestration by unburned, charred material (Verma & Jayakumar, 2012). If elements volatize, they are lost from the immediate environment (e.g., nitrogen) (Caldwell *et al.,* 2002) Nitrogen begins to volatize at 200°C and is completed by about 500°C (figure 1.4). Major elements that persist after a fire event tend to increase in relative concentration as others are lost. Magnesium (Mg), calcium (Ca), and manganese (Mn) volatize at temperatures over 1000°C, meaning they persist after most fire events

10

while phosphorous (P), potassium (K), and sulfur (S) may persist depending on fire temperature (Figure 1.4) (Bodí *et al.,* 2014). Once biomass converts to ash, these major elements enter the soil and become an important source of nutrients for plant growth (Pereira *et al.,* 2012); however, trace element signatures from fire ash are less understood and warrants more investigation.

1.4 Fire Ash Characteristics

Ash is typically described as the residual mineral material left over after burning organic material (Bodí *et al.,* 2014). Though simplistic, this definition leaves out the "altered" organic fraction of ash and the incorporation of foreign materials into the matrix. Therefore a more comprehensive definition of fire ash can be explained as:

> "the particulate residue remaining, or deposited on the ground, from the burning of wildland fuels and consisting of mineral materials and charred organic components" (Bodí *et al.,* 2014).

This definition accounts for (1) an organic component, where organic materials persist as charcoal or soot; (2) an inorganic component, where mineral silicates, oxides, phosphates, carbonate, sulfates and other water soluble elements exist; (3) the ability for *in situ* soil particles to become incorporated into the matrix; and (4) incorporation of *ex situ* materials deposited from the atmosphere (Bodí *et al*., 2014; Campos *et al.,* 2015).

The use of fire ash and biochar as a traditional agricultural soil amendment has been well known for centuries, dating back as far as 2,000 years to the *terra preta* soils of the Amazon basin (Glaser *et al.,* 2001). Pitman (2006) noted fireplace ash as equivalent to a 0-3-14 (N-P-K) fertilizer and used to enrich soils deficient in potassium (K). Farmers in the US also used fireplace ash up to the early 20th century to: preserve meats (mainly using ash from maple and hickory woods), insulate houses for the winter (ash creates a

11

bonding agent for hay fibers in insulation), as an abrasive to clean dishes, and a component in making lard soap (Sloane, 1956). All of these uses stem from unique physical and chemical properties of fire ash.

1.4.1 Color: Color of ash serves as a proxy for combustion completeness and intensity of burning (Úbeda *et al.,* 2009, Bodí *et al.,* 2011 Pereria *et al.,* 2012). Typically "darker" ash indicates incomplete combustion because organic carbon remains, while "lighter" ash indicates only mineral material persists (Bodí *et al.,* 2014). Under a series of different burn intensities, cork oak (*Quercus suber*) ash varied in color from yellow-ish grey at 150°C to red at 200 - 250°C, black at 300°C and grey/white at above 400°C (Úbeda *et al.*, 2009). As fire intensity increases, calcium carbonate, total sulfur, and pH generally increase, but total carbon content, total nitrogen, and total phosphorous decreases (Pereira *et al.,* 2012). Increases of calcium carbonate and decreases in total organic carbon results in the ash turning lighter in color. Dark ash colors also tends to have higher amounts of water extractable Ca, Mg, and K (Pereira *et al.,* 2012). This is likely due to similarities of charred ash to biochar material.

1.4.2 Particle Size and Porosity. Particle size of ash correlates with combustion completeness. Based on control burns of *Eucalyptus radiate,* Bodí *et al.* (2011) found ash of more complete combustion (i.e., lighter in color) tended to be of finer particle size. Between 350 and 700 °C ash tended to become finer as temperature increased. Above 900°C, re- crystallization of calcite and other mineral elements caused particle size to increase (Bodí *et al.,* 2011). Etiegni & Campbell (1991) classified ash composition as 80% particles of less than 1.0 mm and 20% charred organic fragments. The proportion of fine particles and charred fragments is highly dependent on combustion completeness and

fire duration. Bulk density of wood ash is usually lower than that of average mineral soil

due to porosity values of 60-90% (Bodí *et al*., 2014). With high porosity, ash has an

incredible water holding capacity. A given thickness of ash can store water to a depth of

half its thickness before runoff occurs (Bodí *et al*., 2014).

   1.4.3 Chemical Composition: Major minerals present in forest vegetation ash

include: calcite ($CaCO_3$), lime (CaO), riebeckite (($Na,Ca)_2(Fe,Mn)_3Fe_2(Si,Al)_8$),

portlandite ($Ca(OH)_2$), calcium silicate (Ca_2SiO_4), hydrotalcite ($Mg_6Al_{12}CO_3(OH)_{16}$

$\cdot 4H_2O$) and seranditie ($Na(MnCa)_2Si_3O_8(OH)$) (Etiegni & Campbell, 1991; Demeyer *et*

al., 2001). In a sequence of volatilization potential, organic compounds are first to

combust followed by a succession of elements seen in figure 1.4. Alkaline compounds

tend to mineralize into carbonates, converting to hydroxides and oxides under extreme

temperatures (Etiegni & Campbell, 1991). Major elements like magnesium (Mg), calcium

(Ca), potassium (K), phosphorus (P), sodium (Na), sulfur (S), manganese (Mn), iron (Fe),

silicon (Si) and zinc (Zn) have been detected in wood ash (Etiegni & Campbell, 1991;

Demeyer *et al.,* 2001; Bodi *et al*. 2014). Trace elements like arsenic (As), lead (Pb),

nickel (Ni), chromium (Cr), cadmium (Cd), mercury (Hg), vanadium (V), and cobalt (Co)

have been elevated in soils after major forest fire events (Campos *et al.,* 2016).   Pitman

(2006) noted one of the key determinants of ash chemistry is the tree species combusted.

Hardwood species tend to have higher amounts of macronutrients and lower silica

content than ash derived from conifer species. Ash derived from hardwoods often

contains more K, P and Ca and less Si than conifers (Pitman, 2006).

1.5 Project Aim

As field research on fire ash composition focused on ash generated from an aggregate of wood species, the overall objective of this research is to understand if different tree species have different proportions of elements in their respective ash. This research also builds on research by Darley (2017) to try and identify trace element signatures of forest fires in soil.

Presence-absence of trace elements is significant as most ash research only focuses on major element composition (silica, calcium, sodium, iron, magnesium, potassium, and phosphorous), forgetting the potential of trace element signatures. Varying composition among species specific ash will show ash material is *not* homogenous throughout the burnt environment and may not necessarily be bedrock dependent. The ability for certain tree species to sequester specific elements likely influences ash chemistry. This means ash material might be based on the tree species burned and is heterogeneous across the burnt landscape. Research suggests vegetation type plays a key role in ash elemental composition (Bodí *et al.,* 2011; Pererira *et al.,* 2012); however, few compare ash compositions from multiple species from one contiguous forest. Hence, research is needed to see how different tree species contribute different proportions of elements to the ash matrix. Studying ash chemistry provides critical information on rapid biogeochemical conditions post-fire and can help support controlled burn policy. The controlled use of fire can reduce excessive fuel buildup, slow invasive species colonization, and bolster forest health by helping to create a healthy mixed successional forest mosaic.
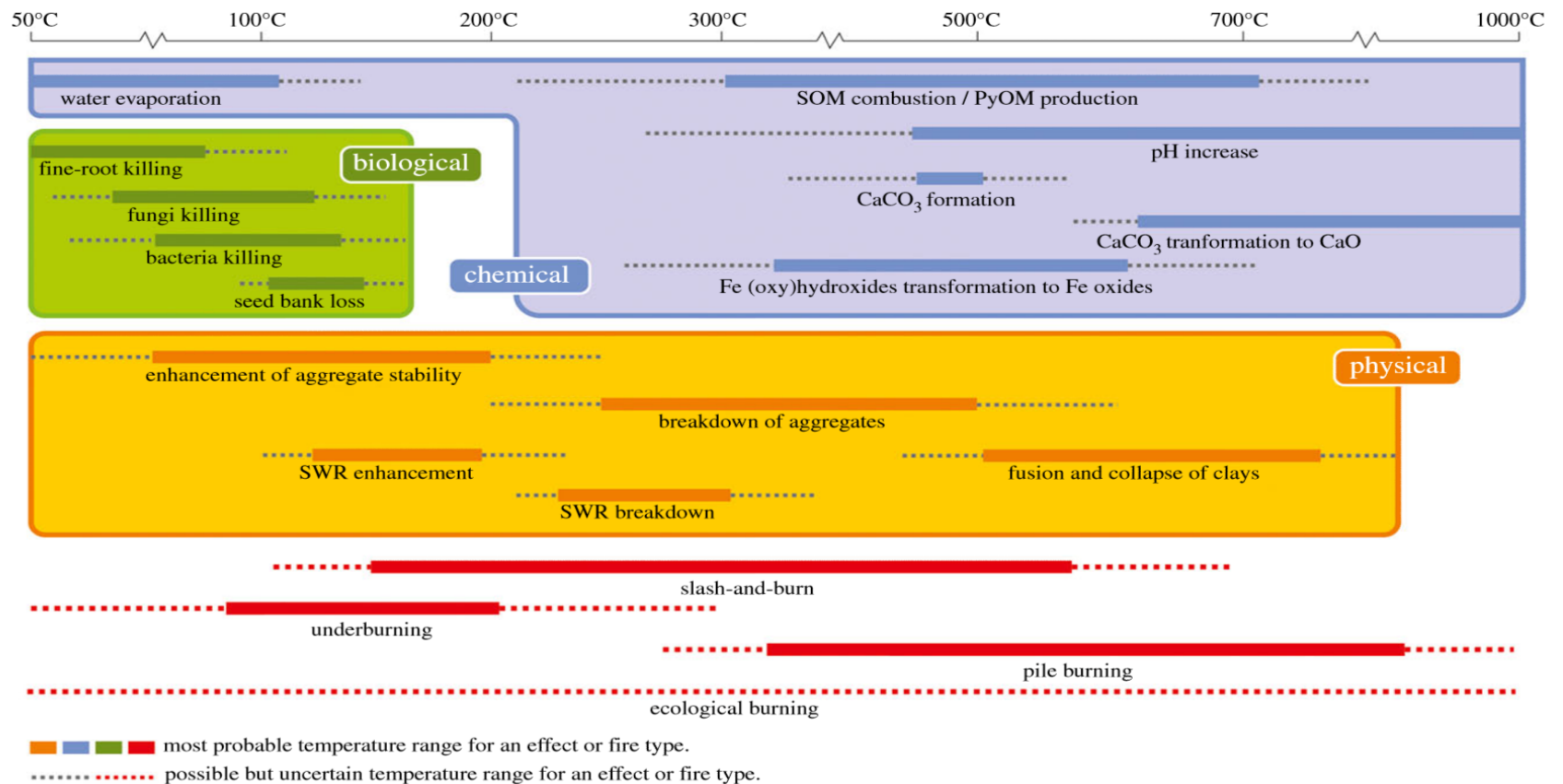
Figure 1.1: General physical, chemical, and biological effects of fire on soils. Figure reproduced from Satin & Doerr (2016). Soil alterations based on burn temperatures near mineral soil surface. Anthropogenic burning activities (under burning, slash-and-burn, pile burns, and ecological burns) superimposed as a reference for different fire types and as a benchmark for burn temperatures. SOM: Soil organic matter; PyOM: Pyrogenic Organic matter (charcoal); SWR: Soil water repellence (Satin & Doerr, 2016).

(a)Fuel Hazards

(b) Fire Risk

R = High

Y = Moderate

G = Low

P = Agricultural

R = High Risk

Y = Moderate Risk

G = Low Risk
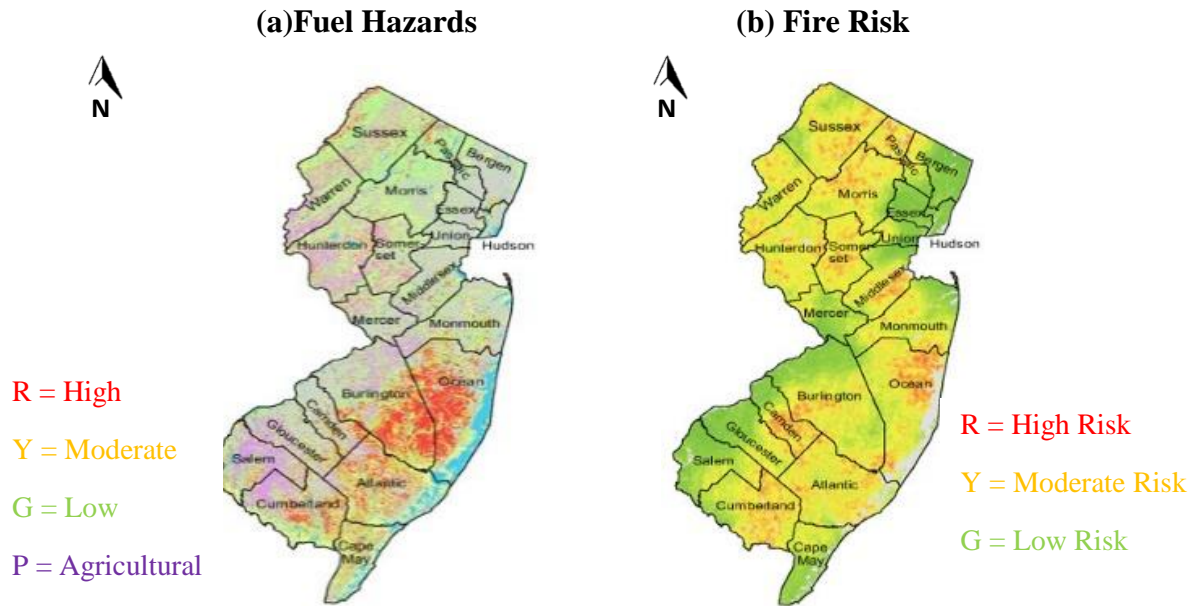
Figure 1.2 Fuel load and fire risk maps of New Jersey. Maps from NJDEP (2014). Map Scale: 1 inch = 100 miles. (a) NJDEP fuel load map of New Jersey. Red indicates high fuel load hazards while green inidcates low hazard. Purple signifies agricultural lands. Elevated fuel loads seem to be conentrated along the Kitattiny ridge (northwest) and the Pine Barrens (southeast). (b) NJDEP Fire risk map. This map accounts for fuel loads and population density near forests. Red = high, yellow = moderate, and green = low risk.
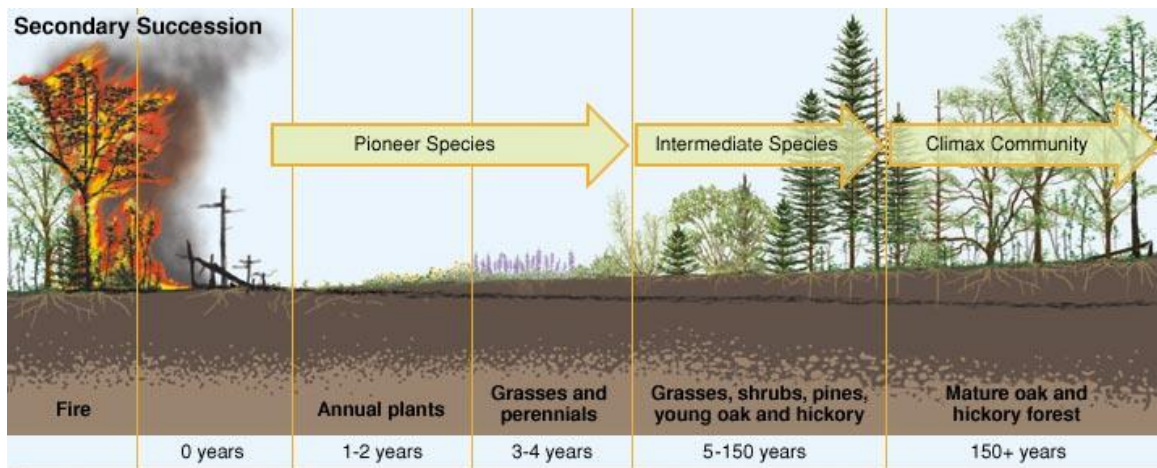
Figure 1.3 Idealized secondary forest succession after a fire event. Composition of surrounding unburnt forest will influence the colonizing vegetation community. Note the "climax community" terminology is misleading as this plant assemblage can still undergo change over time. Removing fire disturbance from "climax community" allows for shade tolerant species to colonize and outcompete species in the initial climax community. Reproduced from Arthur *et al.* (2015).
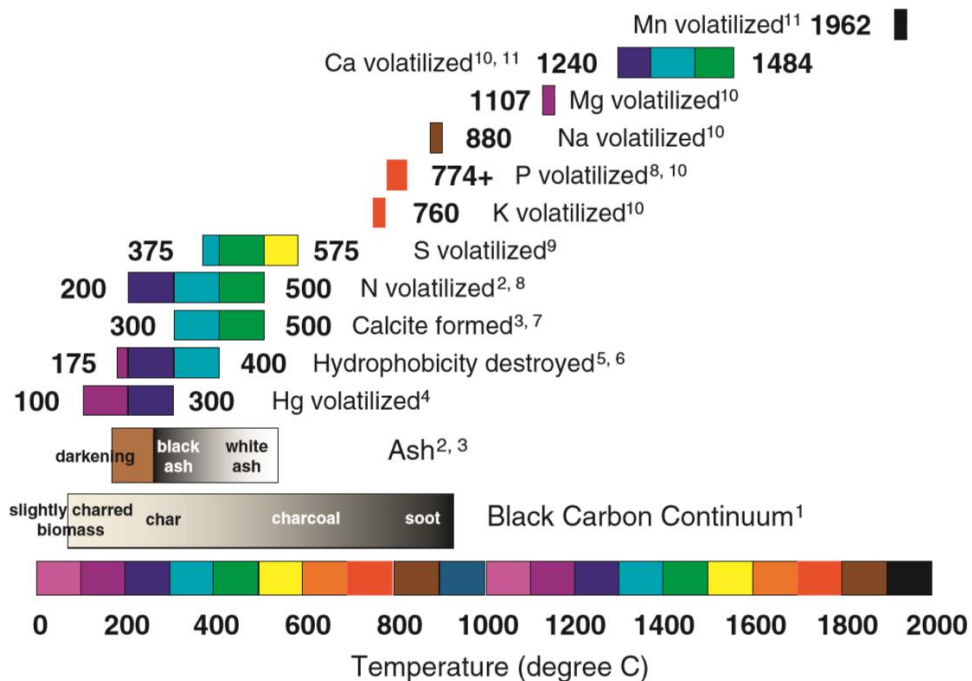
Figure 1.4 Temperature thresholds for major chemical elements in fire ash and soil (Bodí *et al.,* 2014).

Table 1.1: List of invasive insect species and targeted tree genera.

Common name	Latin name	Genera of tree(s) impacted
Two lined chestnut borer	*Agrilus bilineatus*	Oak, beech, hornbeam and chestnuts
Emerald ash borer	*Agrilus planipennis*	Ash (*Fraxinus spp.*)
Hemlock wooly adelgid	*Adelges tsugae*	Hemlock (*Tsuga spp.*)
Asian long horned beetle	*Anoplophora glabripennis*	Maple, birch, elm, ash, poplar, horse chestnut and willow
Spruce bud worms	*Choristoneura spp.*	Spruce (*Picea spp.*)
Southern pine bark beetle	*Dendroctonus frontalis*	Pine (*Pinus spp.*)

** Adapted from Foster & Orwig (2006).

2. METHODS

Fifteen dominant northern New Jersey tree species trees were burned in 1 meter diameter controlled burn plots at the New Jersey School of Conservation in Sandyston, NJ. Temperature readings, along with ash and 10 cm soil cores, were collected and the material analyzed for major, trace, and rare earth elements by Inductively Coupled Mass Spectroscopy (ICP-MS). One plot was left unburned, which acted as a control plot for ash and soil comparisons. Ash color was measured against closet matching Munsell color chip and converted to computer RGB scale by MIT's Munsell Color Pallet (MIT, n.d.). Finally pyrogenic carbon content was assessed by perfoming Loss on Ignition in a muffle furnace on charred ash samples.

2.1 Study Site

Species specific control burns were carried out on a field site at the New Jersey School of Consecration (NJSOC), in Sandyston NJ (Figure 2.1). The school grounds are part of the larger (16,000+ acre) Stokes State Forest in Sussex County New Jersey, and are comprised of uplands and ravines with steep slopes. The uplands consist of mesic mixed oak deciduous hardwoods, while the moist lowlands (ravines or and north facing slopes) have hemlock-mixed deciduous hardwood communities (Collins & Anderson, 1994). Table 2.1 displays tree communities for both forest types.

This area has soils classified in the Swartswood Loam series: moderately deep, well drained, excessively stoney with taxonomic class of Coarse-loamy, mixed, active, mesic Typic Fragiudepts (NRCS Web Soil Survey, n.d.). Parent material consists of coarse-loamy glacial till derived from sandstone and shales deposited after the Wisconsin

glaciation (Harper, 2013; Witte & Epstein, 2005). Deposited surface materials include till, outwash, alluvium, colluvium, talus, and wind-blown sand (Witte & Epstein, 2005). Being derived from glacial materials, soils are expected to have a relatively homogeneous chemical composition. Coarse grained particles are mainly unweathered quartz –pebble conglomerates, quartzite, and red sandstone with finer grained particles consisting of quartz, silt, feldspars, and clay minerals (Witte, 2008). Bedrock lithology consists of the Shawangunk Formation on the uplands and Bloomsburg Formation in the valleys, both Devonian – Silurian in age (Harper, 2013). Most of the bedrock is covered by thick glacial/postglacial deposits (up to 104 meters thick in some areas) and has little influence over present soil development (Witte & Epstein, 2005). Table 2.2a provides a typical soil profile for this area. The soils of the cleared burn site have undergone some anthropogenic disturbance. A soil profile was conducted by Leite *et al.* (2018) prior to this study and the main results appear in table 2.2b.

2.2 Field Methods

Vegetation was collected from dominant tree species found in the approximate area of the burn site. Species collected (n=15) are found in table 2.3 and were chosen based on previously assessed assemblage dominance (Collins & Anderson, 1994) and susceptibility to decline due to storm damage and/or invasive biological agents discussed in section 1.1. All plant nomenclature and taxonomy usage complies with the styles and conventions of *Tropicos,* Missouri Botanical Garden's online botanical database. *Picea abies* (Norway spruce) and *Pinus resinosa* (red / Norway pine) are not listed as dominant plant species in the forest assemblage (table 2.1), but based on site assessments, these

species were apparent in even aged monoculture stands. These monoculture tree communities were likely planted by the Civilian Conservation Corps (CCC) during the 1930's for erosion control, as well as for timber and pulp production (W. Thomas, 2018, personal communication). Unfortunately, these stands have become extremely susceptible to storm damage over the past two decades, contributing to higher fuel loads in the area (figure 2.2). *Pinus resinosa* populations represent a disjoint population at the southern extent of their native range in Northeast and Great Lake forests (Nelson *et al.,* 2014).

Dead or downed wood materials (twigs and branches) were collected and positively identified to the species level. Each wood species was collected from three individual trees greater than 10 cm DBH (diameter at breast height) and had to be separated by 20 meters distance from one another. The 10 cm DBH criterion meant only mature trees were sampled and the distance requirement helped to ensure isolation of individuals and isolated growing conditions. Twenty meter distance among individuals tried to ensure genetic isolation. All collected materials were bundled, tagged, and tarped for three weeks prior to burning. Tarping ensured no additional moisture (via rain), allowed even drying of material, and helped to mimic moisture levels in fuel wood under high fire risk conditions.

The NJSOC field site was chosen as the best site to administer controlled burns due to its openness, isolation from other combustible fuel loads, ease of access to water, and homogeneity of environmental conditions (soils, air flow, and sunlight). A Fire permit was obtained from the director of NJSOC/ fire warden and the permit was granted based on meeting the requirements set forth by N.J.A.C. 13:9 *et al*. (NJ General Forest Fire

Act), N.J.A.C. 7:27 - 2.1 *et seq.* (Control and Prohibition of Open Burning), and N.J.A.C. 5:70-3 *et seq.* (NJ Fire Prevention Code). These regulations limited burning to the designated plots, required an open area with a 10 foot fire break, required at least 5 gallons of water present for each burn, regulated the "fire size" to $2.5 \times 2.5 \times 2$ feet (75cm $\times$ 75cm $\times$ 60cm), required adequate supervision during burning, and only allowed the burning of dead or "downed" vegetation. Figure 2.3 displays the approved NJSOC fire permit.

The field is a disturbed site, once cleared and excavated to lay leaching pipes for a septic leach field some 20 years ago. All excavated materials were replaced *in situ* and any foreign material (stone / gravel used during the building process) remains below sampling depth (W. Thomas, 2018, personal communication). This *ex situ* material has little to no influence on sampled soil composition. Therefore, sampled soils are thought to be "native" and similar in composition to surrounding forest soils. An advantage of sampling soils from this cleared site over sampling soils directly beneath individual species is the elimination of potential bio-augmentation of elements in the soil (i.e., differential elemental sequestration and depletion by certain tree species). The surface soil horizons at this site can represent homogeneous, unmodified elemental availability of the surrounding forest soils.

Sixteen (16) one meter diameter circular plots were created (one for each species plus one control) by removing grass and surrounding each plot with stones to make fire rings. Three meters distance separated each burn plot. On the day of burning (June 27th 2018) the dried wood was stacked within the plots, one species per plot. Dr. Greg Pope, Dr. William Thomas (fire warden), and myself were present to supervise the burns and to

help with data collection (figure 2.4). A Benzomatic MAPP Pro gas torch ignited each of the fires and all fires were left to burn out completely before sampling. No additional fuel was added to any of the fires after the initial set up. A gas torch eliminated the need for foreign materials to start the fires (e.g., pine tinder, paper, and dryer lint) which could have contaminated ash samples and/or altered ash chemistry. The only by-products from burning this torch fuel are water and carbon dioxide. MAPP gas (methylacetylene-propadiene propane) was used over conventional propane as it burns hotter and lends itself to easier ignition of materials.

Fire temperatures were measured for each burn plot using a Fisher Science IR Thermometer (model 42515) at 15 minute intervals for 45 minutes (n=3 readings). This instrument had a reading range of -50 to 800°C at a distance to target ratio of 13:1. Immidiatley after fires burned out (approximately 60 minutes after ignition), surface ash (both mineral and charred) were collected and a 10cm soil core retruieved from the center of each plot (figure 2.5). Ash was cleared from the top of the soil before coring commenced. The top 0-3 cm of the core material was bagged separately from the bottom 3-10 cm, as the top 0-3cm had greater visible organic content. Therefore, sample collection consisted of 32 soil samples and 15 bulk ash samples. According to Table 2.2b, the soil core sampled up to the B horizon. A rain shower occurred at the end of the burn period, which prevented a hydrophobicity test and required all samples to be dried in the laboratory drying oven. All collected materials were labeled and brought back to Montclair State University for laboratory preparation and analysis. After field sample collection water extinguished any remaining embers.

2.3 Laboratory Methods

Sample Prep and Color Analysis. All bulk samples (soil and ash) were thoroughly mixed (individually) to create a homogeneous sample and placed in metal pans for drying. Drying occurred in a Fisher Scientific Isotemp Oven at 95°C for 24 hours to remove any water. Dried samples were then sealed in plastic bags to prevent absorption of atmospheric moisture. After drying, mineral ash samples were matched to closest Munsell color chips (Munsell Company, 2010) and the color recorded in proper hue, value, and chroma notation. Using Massachusetts Institute of Technology's online Munsell Color Pallet (MIT, n.d.), recorded Munsell Colors™ were converted to a Red, Blue, Green (RGB) approximation. The RGB notation provides a system for representing colors on a computer display (MIT, n.d.). RGB values range from 0 to 255 where 0, 0, 0 represents the darkest values and most saturated hues (black) and 255, 255, 255 represents the lightest values and least saturated hues (white) (Kumar & Verma 2010). Mathematical and spatial limitations exist for these color conversions, especially when averaging hue (color) opposites with smallest chroma (intensity) values for grey scale conversion (MIT, n.d.). Python script formula used by the online converter is similar to that of Stokes *et al.* (1996).

Loss on Ignition. Loss on Ignition (LOI), performed in triplicate on the charred ash (black charcoal), assessed the percent remaining pyrogenic carbon content for each species post-fire. Detailed procedures for LOI are outlined by Ben-Dor & Banin (1989). Charcoal was ground into a homogeneous powder using an agate mortar and pestle. A subsample of crushed charred material from each species was placed in a cleaned, dried (24hrs at 95°C), ceramic crucible and weighted to the 0.0001 gram on an analytical

balance. Crucible and samples were then placed into a ThermoScientific Lindberg Blue

muffle furnace and heated to 550°C for 4 hours. Mixed hardwood and conifer saw dust

also underwent LOI (n=6 of each type) to give background carbon content of wood and

to compare total carbon to pyrogenic carbon content. After 4 hours the samples were

removed, set to cool, and reweighed immediately in order to determine the total amount

of organic carbon content. Weighing LOI material as soon as the material cooled

mitigated any mass issues caused by atmospheric moisture adsorption by the sample. A

temperature of 550°C seemed adequate for LOI because according to figure 1.4, the

upper limit of ash color change occurs at this temperature. Above 550°C only white ash

remains, which represents mineral ash with all the organic carbon removed (Bodi *et al.,*

2014). Final data for LOI is presented as percent pyrogenic organic carbon (PyC), as

similarly discussed by Bodi *et al.* (2014) and Bird *et al.* (2015).

   ICP Preparation and Analysis. Preparation of mineral ash and soil samples for ICP-

MS analysis was modified after marine sediment flux fusion procedures developed by

Brachfeld & Gorring (n.d.) at Montclair State University. Sample crushing with an agate

mortar and pestle was not performed because the ash had fine texture and the soils had a

sandy loam texture. A four digit analytical balance was used for mass measurements.

Each sample mass was within 0.0995-0.1005g (0.5% tolerance) and the mass of $LiBO_2$

(flux agent) was within 0.398-0.402g (0.5% tolerance). After attaining the proper mass of

sample and flux, the two materials were thoroughly mixed together and funneled into

graphite crucibles for pyrolysis. Crucibles were placed in a muffle furnace (Thermo

Scientific Lindberg Blue) and heated at 1050°C for 35 minutes. After 35 minutes, a

molten glass bead formed and needed careful swirling within the crucible to pick up any

residual material. Then the crucible was carefully removed from the furnace and the glass

bead poured into Teflon beakers already containing 50mL of trace metal grade 7%

HNO_3. Once the glass bead shattered in the 7% HNO_3, the addition of a magnetic stir bar

helped agitate the sample while the samples were stirred for 20 minutes. After

dissolution, the solution was filtered through Whatman 540 hardened ashless 100mm

filter paper to remove any graphite residue and the solution placed into 60 mL Nalgene™

bottles. Six blanks (consisting of only flux and HNO_3) and ten US Geological Survey

(USGS) and/or National Institute of Standards and Technology (NIST) geochemical

standards (Table 2.4) followed the same procedure. These standards were used for

instrumental calibration and post-processing calibration curves. Since no standards exist

for wood ash, geological and agricultural soil standards had to be used. The standards in

table 2.4 have USGS certified values (Govindaraju, 1989; 1994) for all elements

analyzed.

Placing the fused beads into 50 mL of 7% HNO_3 results in a 500X's dilution, but the

ICP-MS requires a dilution factor of 10,000x's. To create this dilution factor, 0.5 mL of

the 500x's solution and 9.5 mL of 2% HNO_3 was pipetted into 15 mL test tubes and

placed into the auto sampler rack. Major, trace and rare earth element (REE) analysis

took place using a Thermo ICAP Q ICP-MS with ASX-560 auto sampler. Plasma for ICP

forms from the ionization of argon gas ($Ar_{(g)} \rightarrow Ar^+ + e^-$). The instrument exposes argon

gas to pulses of alternating electrical current which causes the ionization reaction to take

place. All samples, blanks, and standards were run in triplicate, with a drift measured

after every fifth sample. Analyzing the drift solution helped correct for any fluctuation of

measurements while the instrument ran. The auto-sampler helped maintain the proper sampling sequence.

ICP-MS reports elemental data in counts per second (CPS) and needs post-processing. At the lab a pre-formatted Microsoft Excel 2017^{TM} template converts CPS data into ppm concentration, calibrated against the geochemical standards. Data processing consisted of drift correction, blank correction, and data conversion using the USGS and NIST geochemical standards for calibration. Elemental data reported for standards (in cps) was plotted against the standard's certified values (Govindaraju, 1989; 1994) for each particular element (in ppm). From the X-Y scatter plots a linear calibration curve (best fit line) approximated a specific elemental concentration (in ppm) based on CPS data. ICP detection limit is suggested at 1 part per billion (ppb) (X. Li, 2019, personal communication).

In order to run all ash samples (n=15), soil samples (n=32), standards (n=10) and blanks (n=12), two rounds of ICP-MS analysis were performed. With two rounds, and three replicates per round, each element had six calibration curves. Table 2.5 reports the coefficient of determination (R^2) values for each calibration curve replicate and the average R^2, pertaining to each element. A calibration R^2 of greater than 0.900 was considered a reliable calibration curve to quantitatively estimate concentration. All elements met this R^2 calibration criteria except for Al_2O_3 (mean $R^2 = 0.614 \pm 0.074$), Ga (mean $R^2 = 0.791 \pm 0.053$), and Pb (mean $R^2 = 0.640 \pm 0.176$). Results pertaining to these few elements might be questionable.

Final data for major elements (SiO_2, TiO_2 Al_2O_3, Fe_2O_3, MnO, MgO, CaO, Na_2O, K_2O, and P_2O_5) were reported as normalized weight percent (wt%); trace elements (Sc,

V, Cr, Co, Ni, Cu, Zn, Ga, Rb, Sr, Y, Zr, Nb, Cs, Ba, Hf, Ta, Pb, Th, and U) were

reported in ppm and rare earth elements (La, Ce, Pr, Nd, Sm, Eu, Gd, Dy, Ho, Er, Tm,

Yb, and Lu) were also reported in normalized ppm. REE's were normalized to chondrite

meteorite concentrations (Masuda *et al.,* 1973) and drift corrected based on procedures by

Cheatham *et al.* (1993). Since all samples had been run in triplicate, the values reported

for each replicate were averaged to attain one concentration value for each element.

These procedures and data display are similar to that of Darley (2017) who compared the

geochemistry of soils inside and outside burned areas of Delaware State Forest,

Pennsylvania. They are also similar to Burton *et al.* (2016) and Campos *et al.* (2016) who

analyzed fire impacted soil, ash, and water for trace elements using ICP-MS

2.4 Statistical Analysis

All statistical analyses used IBM's SPSS™. Multiple regression analyses were only

conducted to determine the coefficients of the linear regression plane for the XYZ color

graph. Statistical significance of RGB values were not necessary as the combination of all

three RGB values always produce one unique color. A scale of 0-255 for Red, Blue, and

Green results in 16,777,216 color combinations. Since the geochemistry data was not

normally distributed, but met assumptions of linearity and homoscedasticity, Spearman's

rank correlations compared all elements against all elements in each respective elemental

grouping (majors, trace, and REE). Separate Spearman's correlation analyses were

completed for ash samples and soil samples. Spearman's correlation coefficient (ρ)

reported for all correlations as well as the statistical significance. Simple analysis of

variance (ANOVA) compared each element concentration in ash versus soil. The lack of

normally distributed data meant only non-parametric ANOVA tests (Mann Whitney U test) could be used for ash-soil comparisons. For consideration of statistical significance, p values had to be below 0.05.
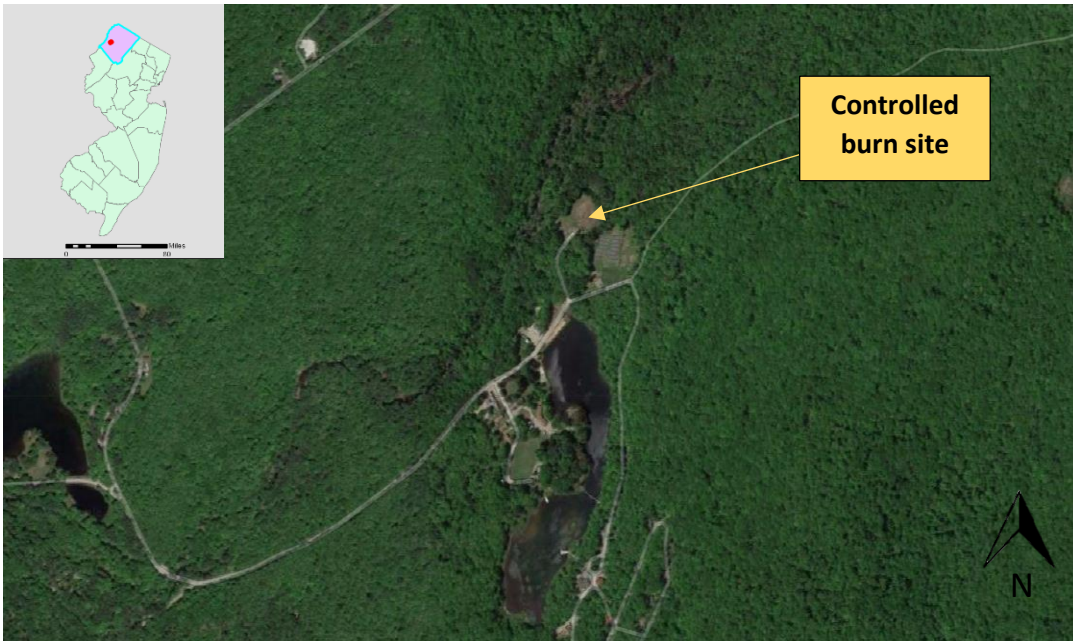
Figure 2.1 Arial view of the New Jersey School of Conservation and location of control burn site (study site). 1 inch = 1000 feet. Data courtesy of NJDEP.

Figure 2.2 Storm damage impact on *Picea abies* as a result of hurricane Sandy (2012) within the grounds of NJSOC**.** Photos by M. Flood (2018).

MONTCLAIR STATE UNIVERSITY

New Jersey School of Conservation

FIRE PERMIT

Permission is granted to: _____*Mike Floods*_____
                                                    (Coordinator Name)
representing: _____*MSU Research*_____
                        (School/Organization if applicable)
for a fire at: _____*Sewer Treatment*_____
                        (NJSOC Location)
between the hours of: _____*8*_____ pm and _____*5*_____ pm

for the date(s) of: _____*6/27*_____

for the purpose of: _____Campfire / *Research*_____
so long as the fire is monitored at all times and is completely extinguished before it is left unattended. This permit must be with you during campfire. Please follow the "leave no trace" rules.

It requires many hours to maintain our wood supply.
PLEASE USE OUR WOOD CONSERVATIVELY

I, _____*Michael Flood*_____
                    (School Coordinator Signature)
agree to the terms and conditions as identified above and will accept full responsibility for the fire.

Issued by: *William H. Thomas*
                William H. Thomas, Ph.D.
                Director, NJSOC

THIS PERMIT IS VALID ONLY FOR FIRES
ON THE CAMPUS OF THE
NEW JERSEYSCHOOLOFCONSERVATION

Figure 2.3. Approved NJSOC fire permit. Controlled burns commenced 6-27-2018.

Figure 2.4 Supervision and temperature recording of species specific control burns. Dr. Greg Pope (blue shirt) and Dr. William Thomas (tan jacket). Photos by M. Flood (2018).

Figure 2.5 Sampling of ash and soil for each controlled burn. Photo by M. Flood (2018).

Table 2.1. Tree assemblages found in mixed oak hardwood forest (uplands) and hemlock -mixed hardwood forests (lowlands) of northern New Jersey. Information adapted from Collins & Anderson (1994).

Mixed Oak Forest (uplands)		Hemlock-Mixed hardwood forest (lowlands)	
Common Name	Latin Name	Common Name	Latin Name
Dominant species		*Dominant species*	
white oak	*Quercus alba*	Eastern hemlock	*Tsuga canadensis*
red oak	*Quercus rubra*		
black oak	*Quercus velutina*		
Other Species		*Other species*	
chestnut oak	*Quercus montana*	red oak	*Quercus rubra*
scarlet oak	*Quercus coccinea*	black oak	*Quercus velutina*
shagbark hickory	*Carya ovata*	black birch	Betula lenta
bitternut hickory	*Carya cordiformis*	yellow Birch	*Betula alleghaniensis*
pignut hickory	*Carya glabra*	basswood	*Tillia americana*
sugar maple	*Acer saccharum*	sugar maple	*Acer saccharum*
red maple	*Acer rubrum*	red maple	*Acer rubrum*
black birch	*Betula lenta*	American beech	*Fagus grandifolia*
American beech	*Fagus grandifolia*		
white ash	*Fraxinus americana*		
black cherry	*Prunus serotina*		
flowering dogwood	*Cornus florida*		
sassafras	*Sassafras albidum*		
ironwood	*Carpinus caroliniana*		

Table 2.2 Soil profile of study site. (a) Typical soil profile as described by the NRCS Web Soil Survey and (b) soil profile as described by Leite (n.d unpubished), who conducted a profile study at the controlled burn site.

(a) NRCS Web Soil Survey			(b) Leite (n.d., unpublished)		
Horizon	Depth (cm)	Texture	Horizon	Depth (cm)	Texture
O_i	0-2.5	Organic	O	0-5	Organic
A	2.5-5	Loam	A	5-7	Sandy loam
E	5-7.5	Sandy loam	AB	7-14	Sandy loam
B_{hs}	7.5 – 10	Gravelly fine sandy loam	B	14-25	Sandy loam
B_W	10 - 54	Gravelly fine sandy loam	B_{T1}	25-50	Sandy loam
B_{x1}	54 -81	Gravelly sandy loam	B_{T2}	50-100	Sandy loam
B_{x2}	81 -152	Gravelly sandy loam	C	100+	
C	152 +				

Table 2.3. Species identified and collected for control burns. Species order alphabetically by scientific name (*) denotes conifer species. Abbreviation after Latin name denotes author who named the tree.

Latin name	Common Name	Latin name	Common Name
Acer saccharum Marsh.	sugar maple	*Populus grandidentata* Michx.	big tooth aspen
Betula alleghaniensis Britton	yellow birch	*Prunus serotina* Ehrh.	black cherry
Betula lenta L.	black birch	*Tsuga canadensis* L.	eastern hemlock*
Fraxinus Americana L.	white ash	*Quercus alba* L.	white oak
Liriodendron tulipifera L.	tulip poplar	*Quercus montana* Willd.	chestnut oak
Picea abies L.	Norway spruce*	*Quercus rubra* L.	red oak
Pinus strobus L.	eastern white pine*	*Quercus velutina* Lam.	black oak
Pinus resinosa Aiton	red pine *		

Table 2.4. USGS and NIST geochemical reference standards used to create elemental calibration curves. Geochemical code, medium type (e.g., rock type) and location of standard extraction are provided (Govindaraju, 1989; 1994).

Standard Code	Type	Location
DNC-1	Dolerite	North Carolina
QLO-1	Quartz Latite	Oregon
W-2	Diabase	Virginia
RGM-1	Rhyolite	California
GSP-2	Granodiorite	Colorado
BIR-1	Basalt	Iceland
AGV-2	Andesite	Oregon
G-2	Granite	Rhode Island
Montana Soil (2711)	Agricultural Soil	Montana
San Joaquin Soil (2709)	Agricultural Soil	California

Table 2.5. Table of calibration curve R^2 values for each element (major, trace, and REE's) for each run. Mean $R^2 \pm$ standard deviation is also reported for accuracy of elemental calibration purposes. Mean calibration curves with R^2 values greater than 0.900 are considered reliable for quantitative estimates of elemental concentration (in ppm). *Rep* = replicate and (**) denotes weak calibration curve.

Majors	Run 1			Run 2			Mean $R^2 \pm$ SD
	Rep 1	*Rep 2*	*Rep 3*	*Rep 1*	*Rep 2*	*Rep 3*	
SiO_2	0.925	0.967	0.965	0.909	0.938	0.916	**0.937 $\pm$ 0.025**
TiO_2	0.992	0.993	0.996	0.972	0.993	0.996	**0.990 $\pm$ 0.009**
Al_2O_3	0.434	0.441	0.775	0.881	0.572	0.582	**0.614 $\pm$ 0.180 ****
Fe_2O_3	0.982	0.99	0.978	0.849	0.969	0.984	**0.959 $\pm$ 0.054**
MnO	0.898	0.904	0.951	0.897	0.918	0.915	**0.914 $\pm$ 0.020**
MgO	0.998	0.99	0.992	0.993	0.999	0.999	**0.995 $\pm$ 0.004**
CaO	0.943	0.955	0.952	0.843	0.95	0.957	**0.933 $\pm$ 0.044**
Na_2O	0.995	0.995	0.996	0.968	0.999	0.982	**0.989 $\pm$ 0.012**
K_2O	0.996	0.956	0.997	0.992	0.995	0.993	**0.988 $\pm$ 0.016**
P_2O_5	0.994	0.988	0.999	0.994	0.996	0.996	**0.995 $\pm$ 0.004**
Trace Elements							
Sc	0.97	0.981	0.989	0.933	0.975	0.975	**0.971 $\pm$ 0.019**
V	0.988	0.987	0.988	0.973	0.981	0.976	**0.982 $\pm$ 0.007**
Cr	0.99	0.986	0.994	0.946	0.979	0.979	**0.979 $\pm$ 0.017**
Co	0.973	0.977	0.98	0.917	0.967	0.966	**0.963 $\pm$ 0.023**
Ni	0.984	0.99	0.992	0.942	0.967	0.97	**0.974 $\pm$ 0.019**
Cu	0.978	0.975	0.981	0.923	0.972	0.966	**0.966 $\pm$ 0.022**
Zn	0.979	0.957	0.968	0.952	0.844	0.865	**0.919 $\pm$ 0.056**
Ga	0.752	0.737	0.756	0.796	0.87	0.834	**0.791 $\pm$ 0.053 ****
Rb	0.99	0.998	0.998	0.999	0.998	0.999	**0.997 $\pm$ 0.003**
Sr 86	0.997	0.996	0.997	0.988	0.991	0.997	**0.995 $\pm$ 0.004**
Sr 88	0.997	0.997	0.998	0.994	0.992	0.997	**0.996 $\pm$ 0.002**
Y	0.963	0.951	0.945	0.828	0.914	0.907	**0.918 $\pm$ 0.049**
Zr	0.988	0.998	0.997	0.996	0.988	0.995	**0.994 $\pm$ 0.004**
Nb	0.992	0.994	0.995	0.99	0.987	0.995	**0.992 $\pm$ 0.003**
Cs	0.999	0.999	0.999	0.999	0.999	0.999	**0.999 $\pm$ 0.000**
Ba 135	0.999	0.999	0.998	0.999	0.992	0.998	**0.998 $\pm$ 0.003**
Ba 137	0.998	0.997	0.998	0.997	0.995	0.998	**0.997 $\pm$ 0.001**
Ba 138	0.999	0.999	0.998	0.996	0.988	0.999	**0.997 $\pm$ 0.004**
Hf	0.999	0.999	0.996	0.993	0.991	0.999	**0.996 $\pm$ 0.004**
Ta	0.991	0.994	0.989	0.994	0.989	0.992	**0.991 $\pm$ 0.003**
Pb	0.607	0.995	0.569	0.546	0.585	0.536	**0.640 $\pm$ 0.176 ****
Th	0.999	0.999	0.999	0.999	0.994	0.999	**0.999 $\pm$ 0.002**
U	0.996	0.998	0.998	0.999	0.999	0.997	**0.998 $\pm$ 0.001**
Rare Earth Elements							
La	0.999	0.999	0.999	0.999	0.991	0.999	**0.998 $\pm$ 0.003**
Ce	0.999	0.999	0.999	0.999	0.998	0.999	**0.999 $\pm$ 0.001**
Pr	0.999	0.999	0.999	0.999	0.999	0.999	**0.999 $\pm$ 0.000**
Nd	0.999	0.999	0.999	0.999	0.999	0.999	**0.999 $\pm$ 0.000**
Sm	0.999	0.999	0.999	0.998	0.996	0.999	**0.998 $\pm$ 0.001**
Eu	0.991	0.985	0.988	0.968	0.97	0.991	**0.982 $\pm$ 0.010**
Gd	0.999	0.998	0.998	0.995	0.992	0.994	**0.996 $\pm$ 0.003**
Tb	0.98	0.983	0.987	0.971	0.96	0.986	**0.978 $\pm$ 0.010**
Dy	0.94	0.97	0.953	0.235	0.925	0.963	**0.946 $\pm$ 0.019**
Ho	0.993	0.96	0.936	0.838	0.927	0.958	**0.935 $\pm$ 0.053**
Er	0.934	0.952	0.941	0.905	0.854	0.834	**0.903 $\pm$ 0.049**
Tm	0.983	0.931	0.938	0.932	0.928	0.965	**0.946 $\pm$ 0.023**
Yb	0.941	0.934	0.957	0.807	0.905	0.929	**0.912 $\pm$ 0.054**
Lu	0.907	0.9488	0.924	0.875	0.8909	0.938	**0.914 $\pm$ 0.028**

3. RESULTS

The most notable result immediately upon burning was the burn temperature for each species (figure 3.2, table 3.1). No fuel material was added to the fires after initial ignition. All burns reached temperatures greater than 500°C, corresponding to fire temperatures generally seen in the western United States (Westerling *et al.,* 2006). *Picea abies* (Norway spruce) had the highest burn temperature at 738.3 $\pm$ 25.5°C while *Betula alleghaniensis* (yellow birch) had the lowest burn temperature at 484.7 $\pm$ 19.2°C. These burn temperatures were significant as they likely influenced the chemical species present in the ash samples (especially mineral ash). Calcite begins to form between 300 and 500°C (figure 1.4) but at temperatures above 550°C calcite and magnesium carbonate decompose to calcium oxide (CaO) and magnesium oxide (MgO) (Kloprogge *et al.*, 2004; Liodakis *et al.*, 2005). Magnesium hydroxide and calcium hydroxide are also present in wood ash and decompose to their respective oxides at temperatures between 390 to 520°C (Liodakis *et al.*, 2005). Reaching temperatures above 500°C likely indicates that hydroxides and carbonates in the mineral ash had already started to decompose to oxides. Thus, the reported results of major element oxides by ICP-MS are representative of major chemical species likely already present in the mineral ash (i.e., minimal carbonate decomposition to oxides during ICP pyrolysis at 1050°C and HNO_3 acid digestion).

Secondly, elemental concentrations within the top 0-3 cm and bottom 3-7 cm soil did not have any statistically significant differences ($p > 0.05$ for all comparisons across all elements). Therefore, the values for each element in top and bottom soil cores (n=16 top and n=16 bottom) were averaged to provide one value per element per soil core (n=16

soil readings). These averaged values were then used for statistical analyses comparing

ash chemistry -- as an aggregate of wood species (n=15) -- against mean soil chemistry,

as an aggregate of soil cores (n=16). Furthermore, soil geochemistry signifies a

background elemental reference to help assess interspecific variation among ash samples.

3.1 Ash Colors

Many works classify ash colors with gray scale values (Roy *et al.* 2010; Bodí *et al*

2014), standard Munsell color notation (Ubeda *et al.,* 2009; Pereira 2012) or hand held

chromameters (Goforth *et al*., 2005). According to table 3.2 the Munsell color notation

and RGB color conversion tended to show ash colors *not* in grey scale, but with yellow,

red, and bluish hues. Mineral ash from individual species tended to vary in hues and

values. *F. americana* (white ash) and *Q. veluntina* (black oak) had the lightest values and

least saturated hues while *Pinus strobus* (eastern white pine) and *T. canadensis* (eastern

hemlock) had the darkest values and most saturated hues (figure 3.1 and table 3.2). Most

ash colors tended to coalesce in one of two color groups (defined by white dashed circles

in figure 3.1). Each of these groups consisted of ash derived from six different species.

Due to the low sample size, little interspecific color variation could be assessed from

within or between groupings. Plotting the RGB equivalent Munsell colors on an XYZ

axis provided an opportunity to develop a linear regression plane to mathematically

explain the color relationships among ash samples (figure 3.1). Multiple regression

analyses were used to generate coefficients for a regression plane equation (figure 3.1).

The linear regression plane had a R^2 value of 0.788 and the equation developed was:

$0.977x - 0.152y + z = 42.918$.

3.2 Pyrogenic Carbon Content (PyC)

Pyrogenic carbon (PyC) is carbon left over from the burning of biomass or the incomplete combustion of organic matter (soot, char, black carbon) (Bird *et al.* 2015). All charred ash underwent loss on ignition (LOI) to determine the percent of carbon remaining among species. All mean percent PyC values were lower than the mixed hardwood and conifer percent carbon content (table 3.3). Generally, wood has a carbon content of about 99% while the PyC content among the charred ash species ranged from 83.8 to 94.2%. *Populus grandidentata* (big tooth aspen) and *Liriodendron tulipifera* (tulip poplar) had the lowest mean PyC % and highest remaining mineral percent. No statistically significant correlations existed between mean PyC% and burn temperature, nor mean PyC% and wood density (ρ<0.400 and p>0.1). The carbon content from sawdust determines the carbon fraction of wood biomass and the PyC of charred ash represents an intermediary stage of carbon content along the biomass to mineral ash conversion. Therefore, the subsequent mineral ash analyses account for about 1-2% of the original wood biomass and 6-16% of the charred ash material. The inorganic portion of wood becomes concentrated after forest fires as carbon volatizes and leaves mineral ash.

3.3 Ash Geochemistry of Major Elements

Silica and calcium oxide contributed the greatest proportions of major oxides in all mineral ash samples (figure 3.2) and had a strong negative correlation with one another (ρ = -.975 and p<0.0005) (table 3.4a). Ash with high percent weights of silica (e.g., derived from *Picea abies*) tended to have less calcium oxide; whereas, ash with high percent weights of calcium oxide (e.g., ash derived from *Q. alba* and *Q. velutina*) tended

to have lower silica content (figure 3.3). Burn temperature does not seem to have an effect on the presence of these two oxides (table 3.4a), indicating oxide contribution to mineral ash is likely dictated based on tree species. More statistically significant correlations existed among oxides in soil samples than among oxides in ash samples (tables 3.4a and 3.4b).

Comparing oxides in ash and soil (figure 3.3), ash was significantly concentrated in MnO, MgO, CaO, K_2O, and P_2O_5 ($p<0.0005$ between all groups). Silica, TiO_2, Al_2O_3, Fe_2O_3, and Na_2O tended to be more abundant in soil than ash samples ($p<0.0005$ between all groups). Interspecific variation among ash samples existed (figure 3.4, table 3.5), with most of the variation found for oxides above the soil average (MnO, MgO, CaO, K_2O and P_2O_5). Less variation existed among ash samples when oxides were below the soil average (TiO_2, Al_2O_3, Fe_2O_3, and Na_2O), with the exception of silica (figure 3.4). Statistically significant oxides above the soil average seemed to vary approximately by tenfold among all ash samples (figure 3.4). Aluminum oxide had a weak calibration curve (table 2.5), so any results for this oxide might be questionable.

3.4 Ash Chemistry of Trace Elements

Many, but not all, trace elements are utilized by plants for metabolic and physiologic function (Raven *et al.*, 2002); therefore, some trace elements are expected in ash samples. As an aggregate of samples, mineral ash tended to be significantly concentrated in Ni, Cu, Zn, Sr, and Ba ($p<0.0005$ for Cu, Zn, Sr, Ba by MannWhitney-U test) above the soil average (figure 3.5). Nickel had the least significant enrichment

among all the statistically significant elements (p = 0.048). Soils had higher

concentrations of Sc, V, Cr, Co, Y, Zr, Nb, Cs, Hf, Ta, Pb, Th, and U than ash (p<0.0005

for Sc, V, Cr, Y, Zr, Cs, Hf, Ta, Th, and U; p= 0.001 for Nb and p= 0.004 for Pb). No

statistically significant relationship existed for Ga or Rb between ash and soil. Weak

calibration curves are noted for Ga and Pb (table 3.5); caution should be exercised when

interpreting the results of these two elements.

As with major oxides, much interspecific variation seemed to exist among ash

samples in regards to certain trace elements (table 3.6). Of the enriched elements, Zn, Sr

and Ba had the greatest variation, while Ni and Cu had less variation among ash species

(figure 3.6). All species tended to yield ash with high concentrations of Zn, Sr, and Ba.

The only exception was ash from *Q. alba* (white oak), which had a lower zinc

concentration than the other species and well below the soil mean for Zn. Ash derived

from *Populus grandidenta, B.lenta* (black birch) and *B. alleghaniensis* had greatest

enrichment above the soil mean in Zn and Ba, while ash from *F. americana* had the

greatest concentration in Cu and Sr. *Populus grandidenta* also had a significant enriched

in Ni, well above the soil mean and many other species.

Separate correlation analyses for ash and soil samples of all trace elements against

all trace elements are shown in table 3.7 a and b. More statistically significant

correlations existed among trace elements in soil than in ash samples. Of particular

interest were the positive correlations between Ni and Zn (r=0.606, p<0.05), Ni and Ba

(r=0.614, p<0.05), and Zn and Ba (r=0.870, p<0.01) in the mineral ash. These elemental

correlations only appeared in the ash (table 3.7 a&b) and showed a statistically significant

enrichment in ash over soil.

41

3.5 Ash Geochemistry of Rare Earth Elements

Rare earth elements (REE's) are a group of 14 elements in the lanthanide series, typically found at low concentrations in the soil environment and bound to silicate, phosphate, and carbonate minerals (Tyler, 2004; Ramos *et al.,* 2016). All these elements were found more concentrated in ash samples and had greater concentrations than the background soil mean (figure 3.6) ($p<0.0005$ for all REE's). Light rare earth elements (LREE's = La, Ce, Pr, Nd, Sm, Eu, Gd) had greater concentrations in both ash and soil than the heavy rare earth element (HREEs = Tb, Dy, Ho, Er, Tm, Yb, Lu) (figure 3.6, table 3.8). With all REE's concentrated in ash samples, a concentration factor was calculated between ash and soil (table 3.9). The mean concentration for a specific REE in the ash was divided by the same mean REE concentration in the soil. These calculations yielded concentration factors of 10-15 times among all REE's (table 3.9). Therefore, ash samples were 10-15 times more concentrated in all REE's than the background soil average. Additionally, a slight decrease in europium (Eu) seemed to appear in the ash samples, but not in the soil samples (figure 3.6). This is denoted by the slight dip in the Eu mean when comparing neighboring REE (Sm and Gd) on figure 3.6.

High interspecific variation occurred for all REEs (table 3.8, figure 3.7 and figure 3.8). Ash from *Populus grandidentata* had the highest concentration of all LREE's except for Ce (figure 3.7) and highest concentration of Tb, Dy, Ho of the HREEs (figure 3.8). *Picea abies* ash had higher concentrations than *Populus grandidentata* ash in the remaining HREEs (Er, Tm, Yb, and Lu). Ash samples from *Q. velutina, Q. alba, B. alleghaniensis,* and *F. americana* appeared less concentrated in all REE concentrations

than other species, but still had higher concentrations than the soil average (figure 3.7 and

figure 3.8).

REE correlations of ash and soil appear in tables 3.10a and 3.10b. All REEs had a

significant positive correlation to one another in both ash and soil samples (p<0.05).

Similarly when conducting a correlation analysis of all major oxides against all REEs

(table 3.10) in ash samples (n=15) only CaO and SiO_2 had statistically significant

correlations with <u>every</u> REEs. All REEs had a statistically significant negative correlation

with CaO (p<0.05), while all REEs had a statistically significant positive correlation with

SiO_2 (p<0.05) (table 3.11). It is noteworthy to re-mention SiO_2 and CaO had a

statistically negative relationship with one another in ash samples (table 3.4a, figure 3.2).
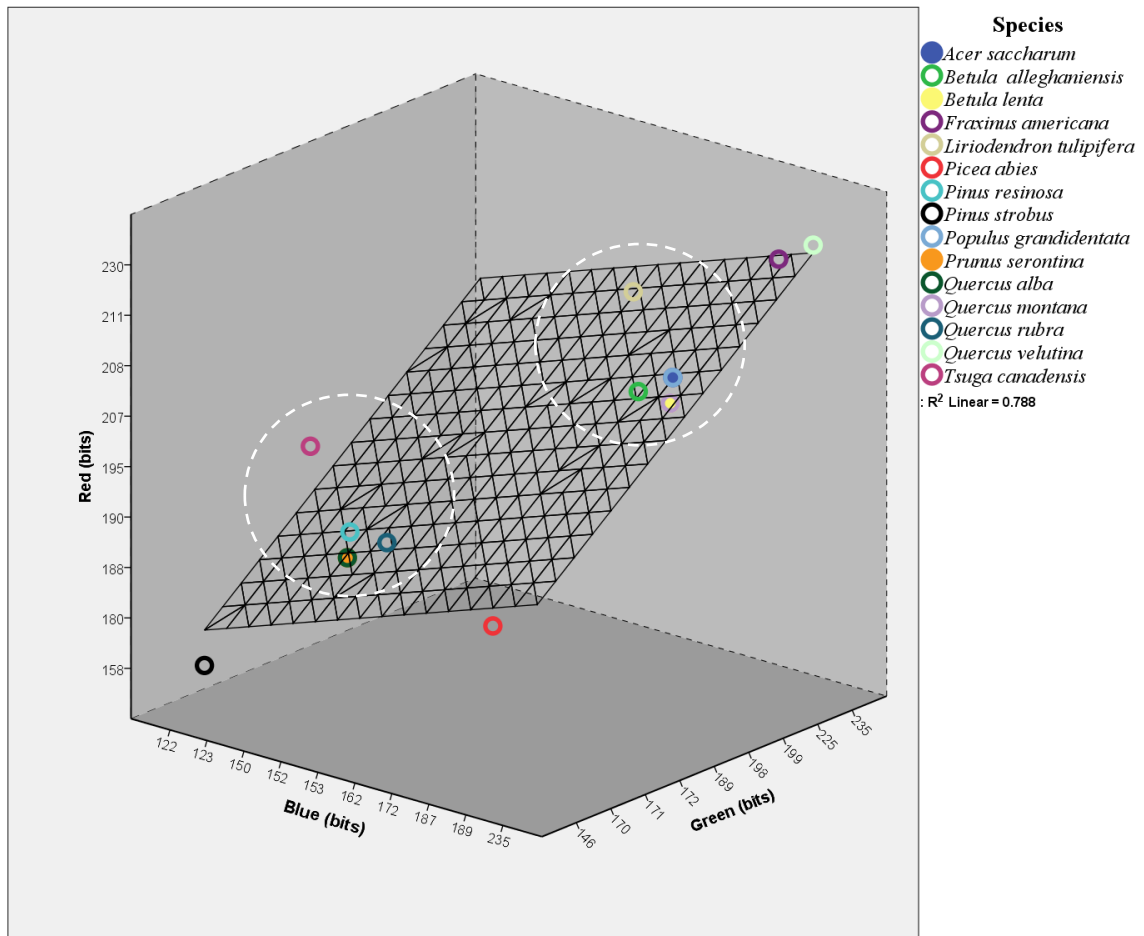
Figure 3. 1 Red, Blue, Green computer color values (in bits) plotted on an XYZ graph. Each ash sample is labeled by species (n=15). Increasing RGB values indicate less saturated hues and lighter values. Note: Some symbols filled in for ease of viewing on the graph. *F. americana* (white ash) and *Q. veluntina* (black oak) tended to have the least saturated hues and lightest values while *Pinus strobus* (eastern white pine) and *T. canadensis* (eastern hemlock) tended to have the deepest hue saturation and darkest values. Most ash colors tended to coalesce in one of two color saturation groups (defined by white dashed circles, n=6 species per group). The equation of the regression plane (in standard form) is $0.977x - 0.152y + z = 42.918$ and has an R^2 value of 0.788. This regression plane provides a mathematical representation of ash color variation based on tree species burned where X=Red, Y=Green, and Z=Blue.
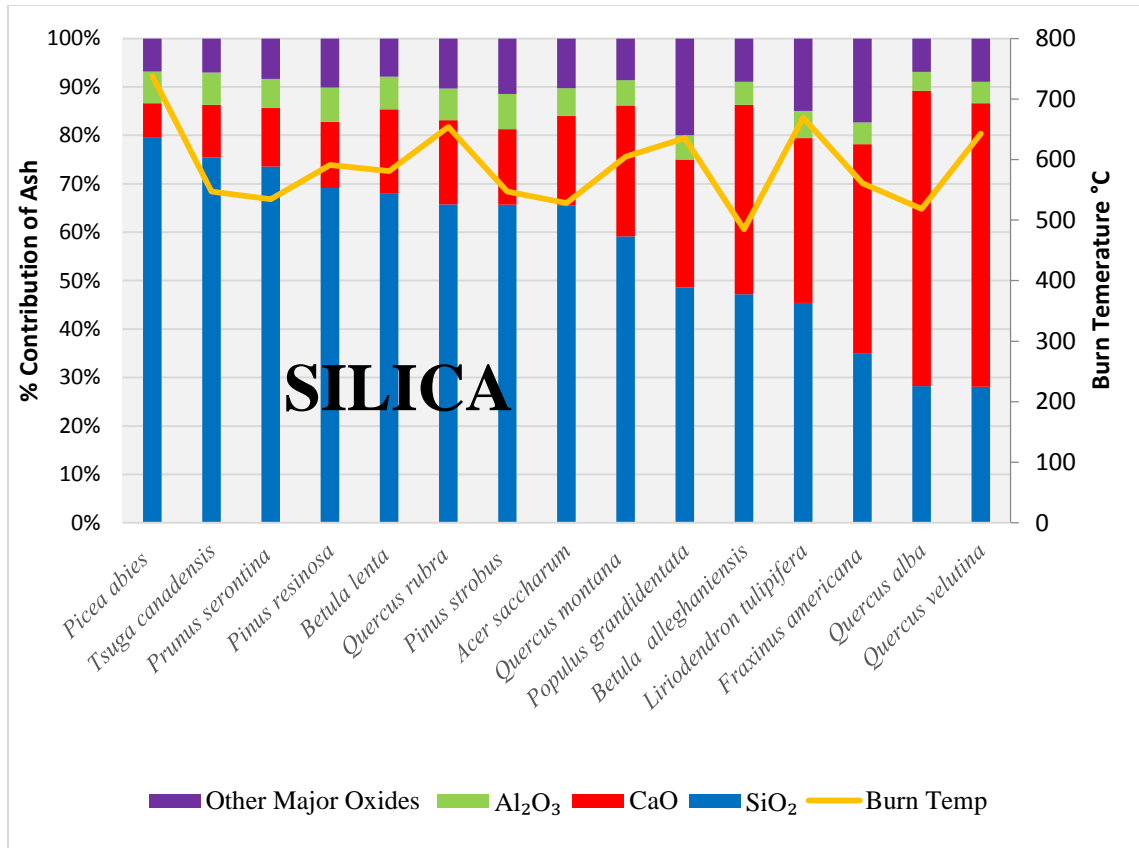
Figure 3. 2 Stacked bar graph of silica (blue), calcium oxide (red), and aluminum oxide (green) percent weights per species specific ash. Wood ash ordered by descending silica content. The category "other major oxides" includes Fe_2O_3, MnO, MgO, Na_2O K_2O, and P_2O_5. Line graph and secondary axis (right) indicates average burn temperature per species in °C. A strong negative Spearman's correlation existed between silica and calcium oxide (ρ = - .975 and p<0.0005). Burn temperature did not seem to influence oxide presence (table 3.4a). *Populus grandidentata* (big tooth aspen) and *F. americana* (white ash) had the greatest percentage of "other" major oxides contributing to the ash matrix.
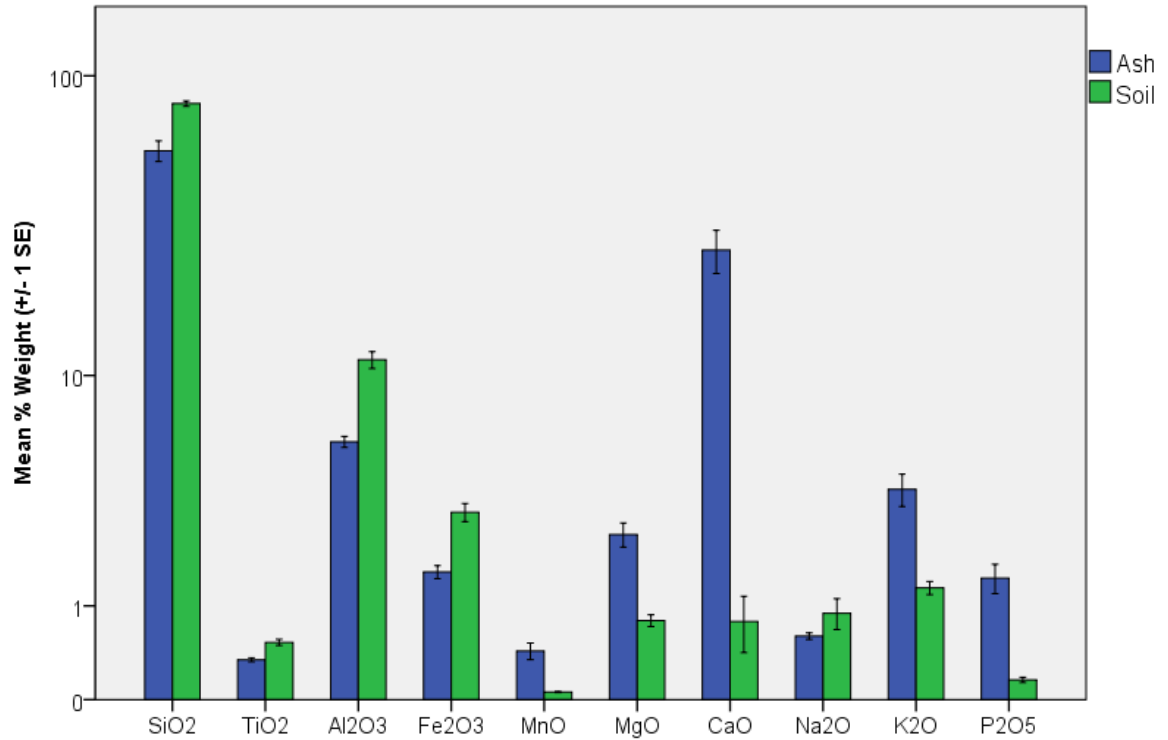
Figure 3. 3 Comparison of major oxide percent weight in ash versus soil samples. Ash samples (n=15) are statistically significantly concentrated in MnO, MgO, CaO, K_2O, and P_2O_5 (p<0.0005 between each comparison) over soil samples (n=16). Note: blue bars indicate mean ash percent weights and green bars indicate mean soil percent weights per oxide. Error bars indicate $\pm$ 1 SE. Y axis in log scale.
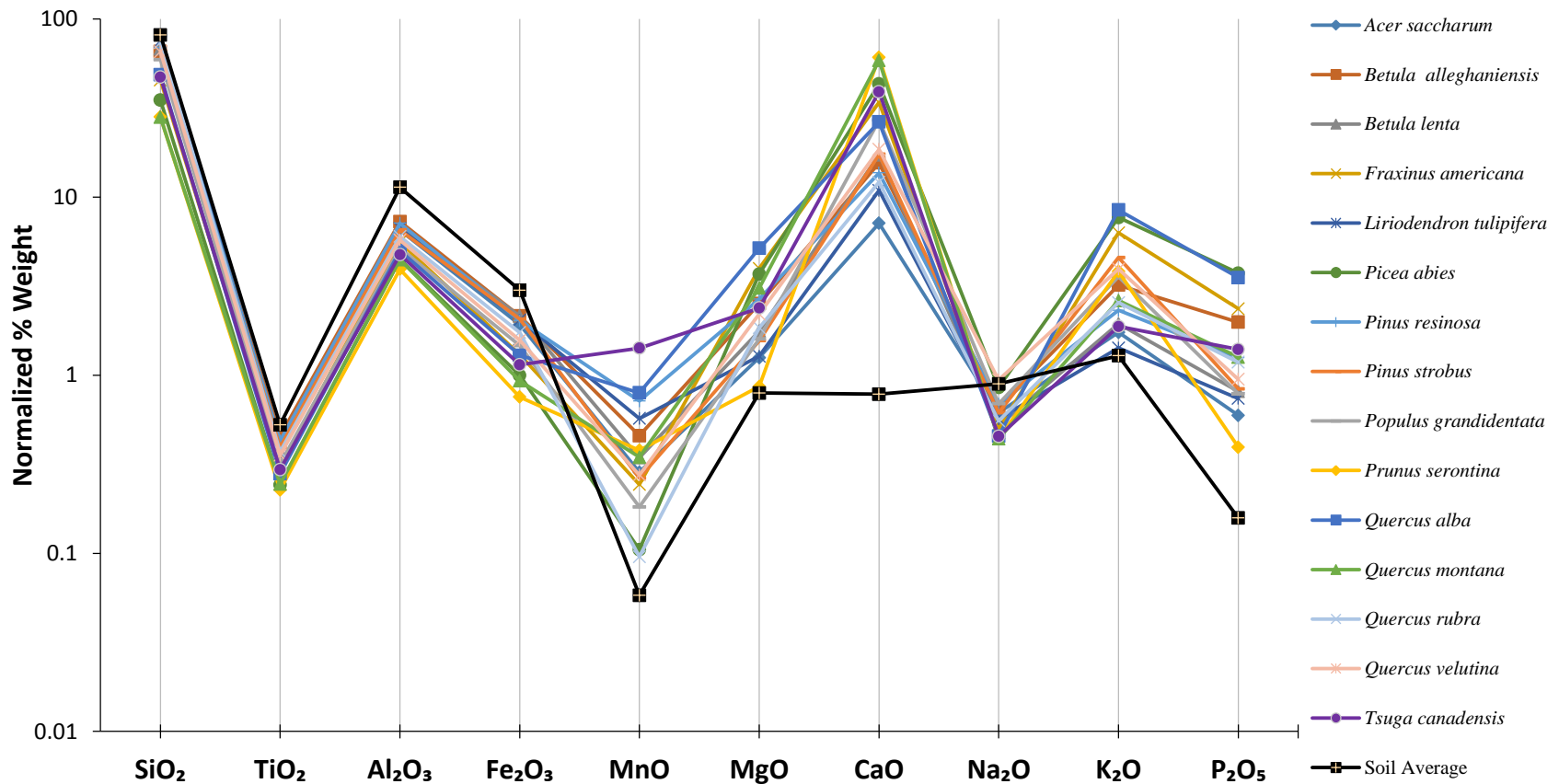
Figure 3.4 Interspecific variation of major oxide percent weight among species specific ash samples. Colored lines represent percent weight data of ash from different tree species. Black line represents averaged percent weight for soil. Y axis in logarithmic scale. A tenfold variation in percent weight of oxides exists among tree species where oxides were above the soil average (MnO, MgO, CaO, K_2O, and P_2O_5). Oxides below the soil average had less variability among species specific ash samples.
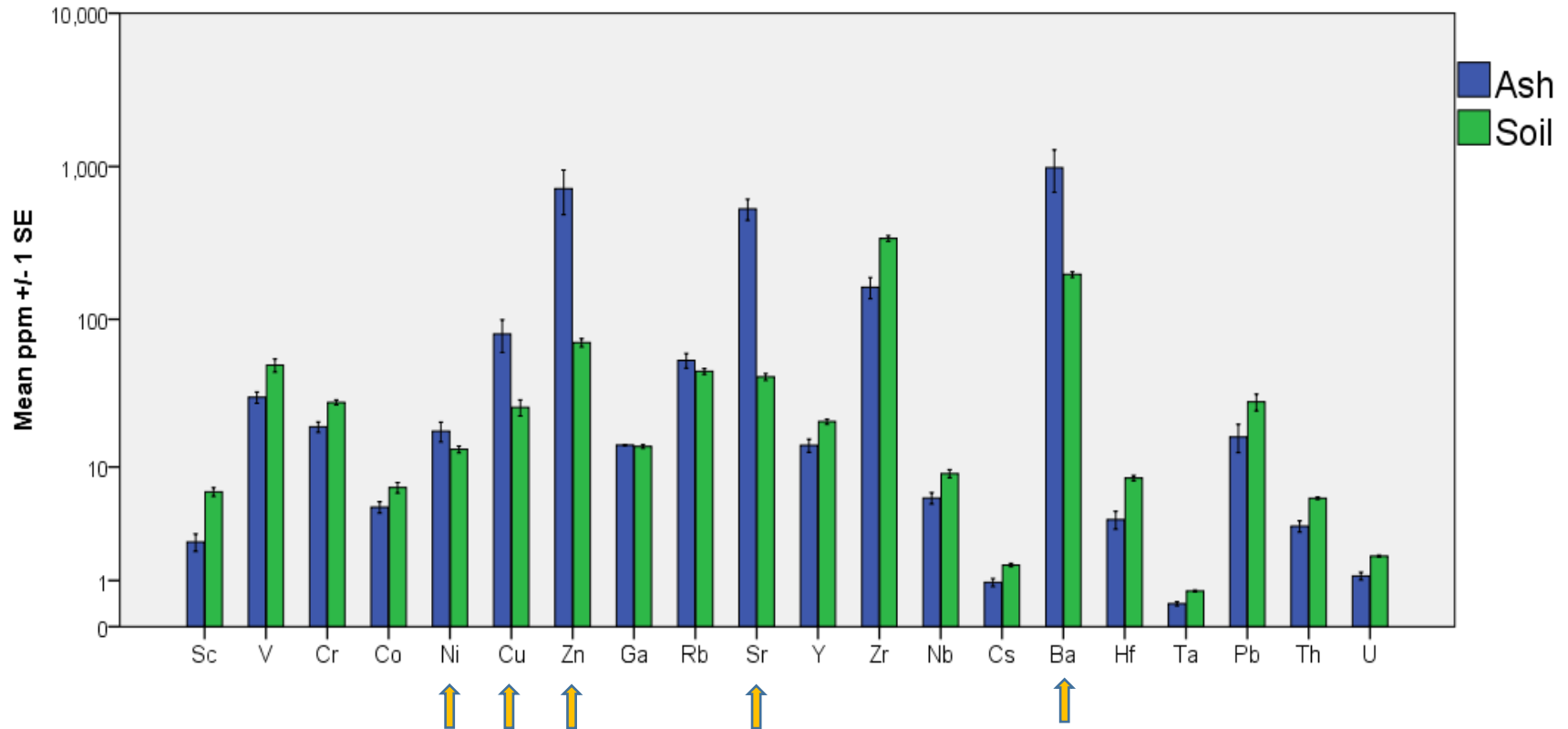
Figure 3. 5 Comparison of trace elements (ppm) in ash versus soil samples. Error bars indicate $\pm$ 1 standard error and Y axis in log scale. Elements listed by increasing atomic weight. Ash samples (n=15) were statistically significantly enriched in Ni, Cu, Zn, Sr, and Ba (p = 0.048 for Ni and p<0.0005 for Cu, Zn, Sr, Ba) over soil samples (n=16). Soil samples had statistically greater concentrations of Sc, V, Cr, Co, Y, Zr, Nb, Cs, Hf, Ta, Pb, Th, U than ash (p<.05). Ga and Rb did not have a statistical difference in concertation between ash and soil. Note: blue bars indicate mean ash ppm and green bars indicate mean soil ppm for each respective element.
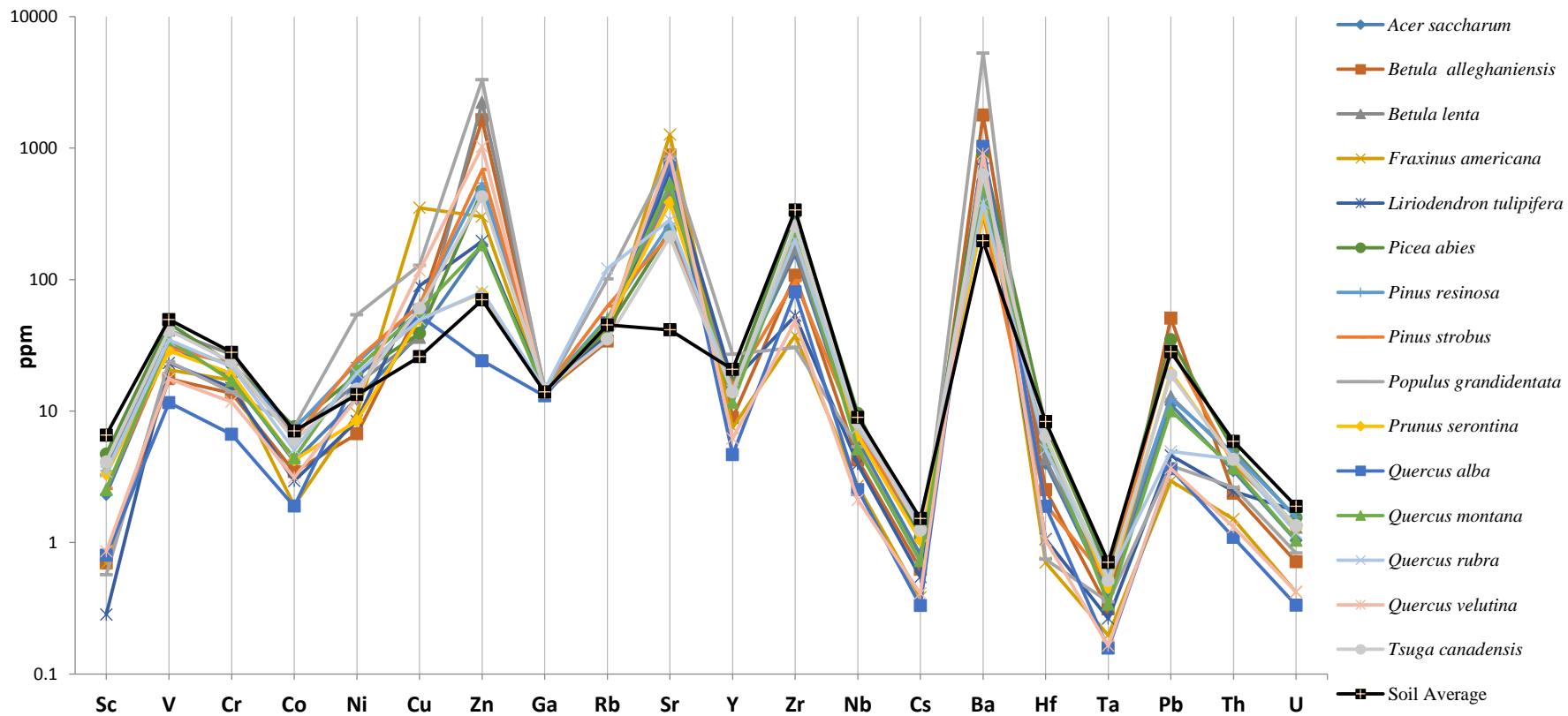
Figure 3. 6 Interspecific variation of trace elements (in ppm) among ash samples. Colored lines represent ash derived from certain tree species. Black line represents averaged ppm for each element in the soil. Y axis in logarithmic scale. Elements listed by increasing atomic weight. Ash derived from *Populus grandidenta, B.lenta* and *B. alleghaniensis* seem to be highly concentrated in Zn and Ba, above the soil mean. Ash from *F. Americana* seems to be concentrated in Cu and Sr and *Populus grandidenta* enriched in Ni. Ash derived from all species seemed significantly enriched in Cu, Zn, Sr, and Ba, above the soil mean. A few ash samples from certain tree species seem enriched in Ni and Rb, above the soil mean. Elements listed by increasing atomic weight.
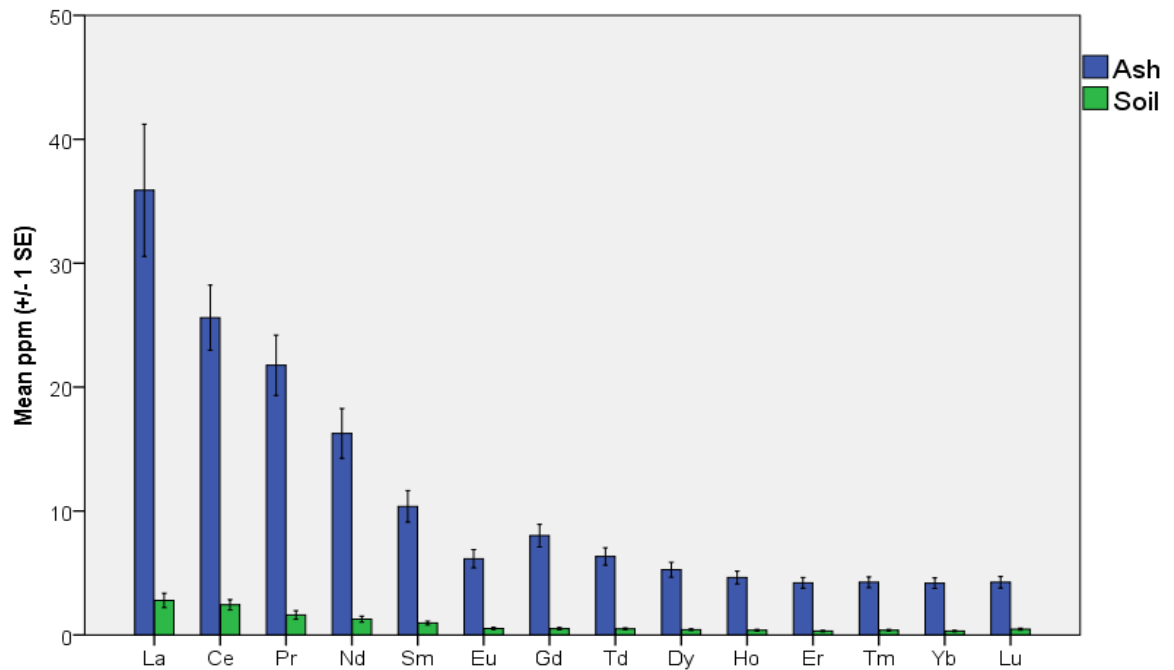
Figure 3. 7 Comparison of rare earth element concentrations (ppm) in ash versus soil samples. Elements ordered by increasing atomic weight. Error bars indicate $\pm$ 1 standard error. Wood ash (n=15) was statistically significantly concentrated in all rare earth elements (p<0.0005 for all REE's) above background soil levels (n=16). A negative europium (Eu) anomaly seemed to appear in the ash samples, but not in soil samples. The negative Eu anomaly is denoted by the slight dip in mean Eu concentration when in comparison to neighboring REE's (Sm and Gd).
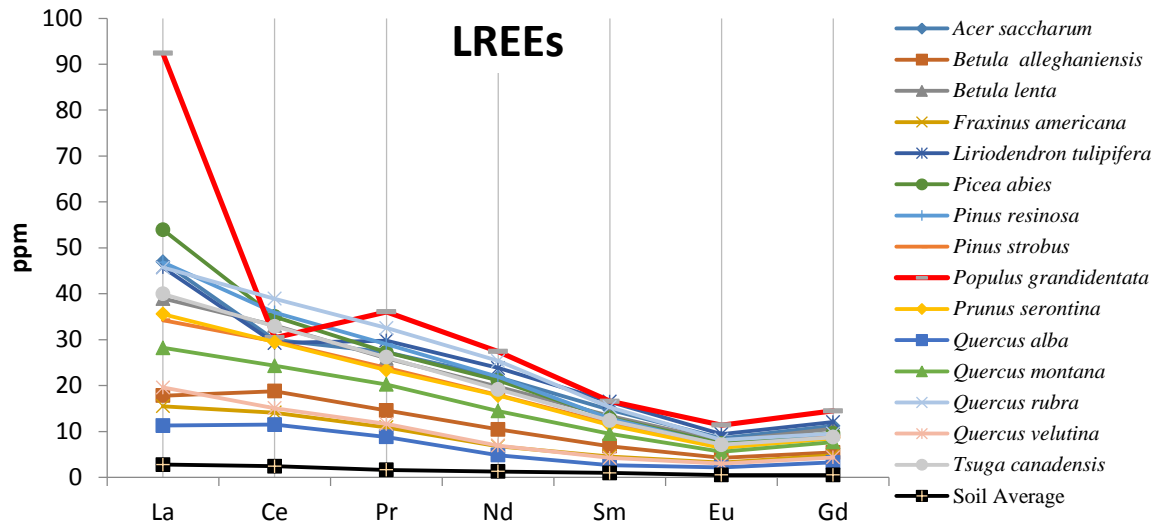
Figure 3. 8 Interspecific variation of light rare earth elements (LREEs) elements among ash samples. Colored lines denotes ash from certain tree species. Soil average plotted in black**.** Elements listed by increasing atomic weight. *Populus grandidentata* seemed to have the highest concentration of LREE's except for Ce, while *Q. velutina, Q. alba, B. alleghaniensis, F. americana* and seem to deviate lower in all LREE concentrations among other species, but were still much greater than the soil average.
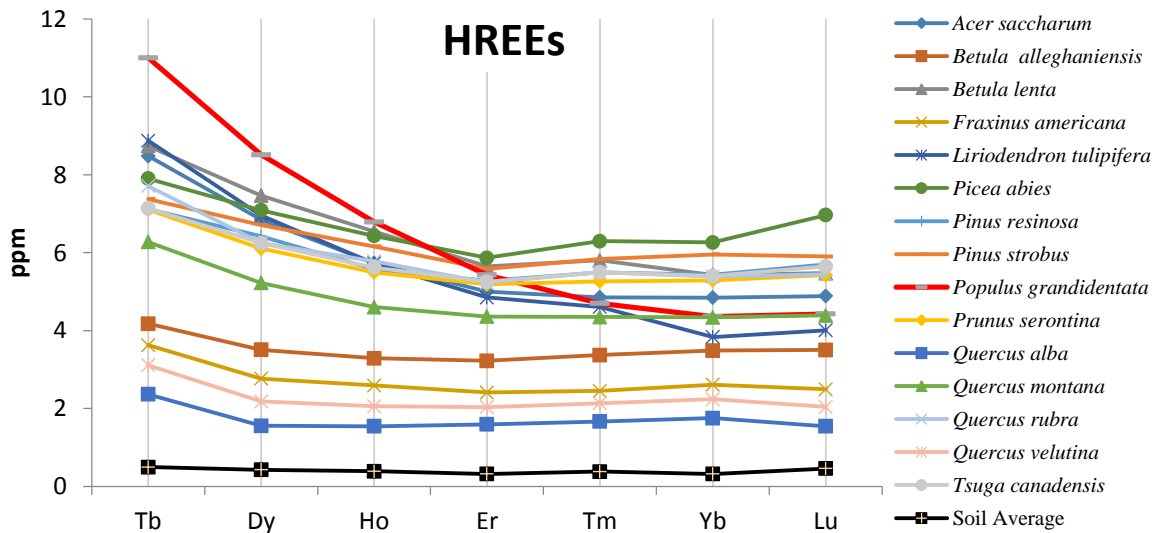
Figure 3. 9 Interspecific variation of heavy rare earth elements (HREEs) among ash samples. Colored lines denotes ash from certain tree species. Soil average plotted in black. Elements listed by increasing atomic weight. *Populus grandidentata* had the highest concentration of Tb, Dy, Ho, with *Picea abies* having the highest concentration in Er, Tm, Yb, and Lu. *Q. velutina, Q. alba, B. alleghaniensis, F. americana* seem to deviate lower in all HREE concentrations among other species, but were still greater than the soil average.

51

Table 3.1 Burn temperatures (± SD) of species specific controlled burns and control. Control readings represent ambient soil conditions. Species listed in descending temperature order (n=3 readings per burn site). Most burn temperatures were greater than 500°C which corresponds to a high intensity forest fire.

Species		Mean Burn Temperature °C ± SE
Picea abies	Norway spruce	738.3 ± 25.5
Liriodendron tulipifera	tulip poplar	669.3 ± 35.0
Quercus rubra	red oak	653.7 ± 7.9
Quercus velutina	black oak	643.0 ± 28.0
Populus grandidentata	big tooth aspen	635.7 ± 37.9
Pinus strobus	eastern white pine	633.3 ± 74.2
Quercus montana	chestnut oak	605.0 ± 122.6
Pinus resinosa	red pine	591.0 ± 13.0
Betula lenta	black birch	581.0 ± 72.9
Fraxinus americana	white ash	561.0 ± 157.9
Tsuga canadensis	eastern hemlock	547.0 ± 104.3
Prunus serontina	black cherry	534.3 ± 64.3
Acer saccharum	sugar maple	528.0 ± 71.8
Quercus alba	white oak	518.7 ± 100.3
Betula alleghaniensis	yellow birch	484.7 ± 19.2
CONTROL (ambient)		33.2 ± .60

Table 3. 2 Munsell color notation, Red, Blue, Green (RGB) color equivalent, and computer generated color for mineral ash samples. Units of RBG units are in computer bits (0-255). Species listed in alphabetical order. RGB conversion performed using MIT's online Munsell color pallet (MIT, n.d.). Species listed in alphabetical order based on Latin name. *F. americana* (white ash) and *Q. veluntina* (black oak) tended to have the least saturated hues and lightest values while *Pinus strobus* (eastern white pine) and *T. canadensis* (eastern hemlock) tended to have the deepest hue saturation and darkest values.

Species	Munsell color	Red (R)	Green (G)	Blue (B)	Generated color
Acer saccharum	7.5 YR 8/1	208	198	189	
Betula alleghaniensis	7.5 YR 8/1	208	198	189	
Betula lenta	10 YR 8/1	207	199	187	
Fraxinus americana	N7/	230	225	235	
Liriodendron tulipifera	2.5 Y 8/2	211	199	172	
Picea abies	10 YR 7/1	180	172	162	
Pinus resinosa	7.5 YR 7/2	190	170	152	
Pinus strobus	2.5 Y 6/2	158	146	122	
Populus grandidentata	7.5 YR 8/1	208	198	189	
Prunus serontina	10 YR 7/2	188	171	150	
Quercus alba	10 YR 7/2	188	171	150	
Quercus montana	10 YR 8/1	207	199	187	
Quercus rubra	7.5 YR 7/2	190	170	153	
Quercus velutina	N8/	230	235	235	
Tsuga canadensis	2.5 Y 7/4	195	171	123	
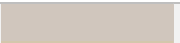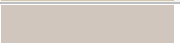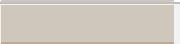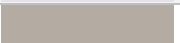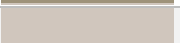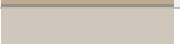
Table 3. 3. Mean percent pyrogenic carbon and remaining mineral material in charred ash samples (n=3 per species). Sawdust samples acted as a background of total carbon content of wood. All mean percent PyC values are lower than the mixed hardwood and conifer percent carbon content, indicating some organic material volatized during the production of charred ash. *Populus grandidentata* and *Liriodendron tulipifera* had the lowest mean PyC% and highest % remaining material (mineral %), indicating these species were more completely combusted than others. No statistically significant correlation existed between mean PyC% and burn temperature, nor mean PyC% and wood density ($\rho<0.400$ and $p>0.1$)

	Mean PyC%	Mean Mineral %	$\pm$ SE
Acer saccharum	94.0	6.0	0.8
Betula alleghaniensis	90.4	9.6	0.7
Betula lenta	93.6	6.4	1.1
Fraxinus americana	92.3	7.7	1.4
Liriodendron tulipifera	85.4	14.6	1.7
Picea abies	93.6	6.4	0.4
Pinus resinosa	94.3	5.7	0.5
Pinus strobus	94.2	5.8	0.3
Populus grandidentata	83.8	16.2	0.5
Prunus serontina	92.5	7.5	0.3
Quercus alba	92.4	7.6	0.7
Quercus montana	86.9	13.1	0.4
Quercus rubra	90.5	9.5	1.4
Quercus velutina	87.3	12.7	1.1
Tsuga canadensis	93.5	6.5	0.6
Mixed Hardwood (n=6)	99.6	0.4	0.0
Conifer (n=6)	99.0	1.0	0.4

Table 3. 4 Correlation matrix of (a) major oxides in ash (n=15) and (b) major oxides in soil (n= 16). Spearman's correlation coefficient (ρ) given along with statistical significance. Statistically significant correlations are in bold font. More statistically significant correlations existed among elements in soil than elements in ash.

(a) Oxide Correlations in Ash										
	SiO_2	CaO	Al_2O_3	TiO_2	Fe_2O_3	MnO	MgO	Na_2O	K_2O	P_2O_5	Burn temp
SiO_2	1									
CaO	**-.975**[**]	1								
Al_2O_3	**.869**[**]	**-.880**[**]	1							
TiO_2	**.920**[**]	**-.902**[**]	**.961**[**]	1						
Fe_2O_3	**.911**[**]	**-.910**[**]	**.977**[**]	**.947**[**]	1					
MnO	-.077	.073	-.063	-.026	-.084	1				
MgO	-.408	.213	-.249	-.375	-.331	.178	1			
Na_2O	.293	-.338	.231	.263	.228	-.386	-.050	1		
K_2O	-.479	.293	-.420	**-0.513**	-.434	-.176	**.752**[**]	.141	1	
P_2O_5	-.388	.185	-.260	-.363	-.317	.068	**.897**[**]	.112	**.826**[**]	1
Burn temp	.128	-.178	.181	.170	.162	-.329	.194	-.128	.184	.057	1

(b) Oxide Correlations in Soil										
	SiO_2	CaO	Al_2O_3	TiO_2	Fe_2O_3	MnO	MgO	Na_2O	K_2O	P_2O_5	Burn Temp
SiO_2	1									
CaO	**-.931**[**]	1								
Al_2O_3	**-.839**[**]	**0.605**	1							
TiO_2	**-.820**[**]	**.923**[**]	.398	1						
Fe_2O_3	**-.927**[**]	**.947**[**]	**0.598**	**.947**[**]	1					
MnO	**-.632**[**]	**.712**[**]	.228	**.832**[**]	**.788**[**]	1				
MgO	**-.923**[**]	**.946**[**]	**0.593**	**.953**[**]	**.984**[**]	**.834**[**]	1			
Na_2O	**-.860**[**]	**.974**[**]	.449	**.963**[**]	**.952**[**]	**.805**[**]	**.948**[**]	1		
K_2O	**-.829**[**]	**.919**[**]	.407	**.975**[**]	**.961**[**]	**.876**[**]	**.961**[**]	**.967**[**]	1	
P_2O_5	**-.875**[**]	**.953**[**]	**0.509**	**.931**[**]	**.933**[**]	**.809**[**]	**.945**[**]	**.955**[**]	**.946**[**]	1
Burn temp	--	--	--	--	--	--	--	--	--	--	1

Bold font and (**) = Correlation is significant at the 0.01 level (2-tailed).
Bold Font = Correlation is significant at the 0.05 level (2-tailed).

Table 3. 5. Mean normalized oxide percent weights of major elemetns in ash per tree species (± SE) and soil average (n=3 reading per oxide per species). Species listed in alphabetical order by Latin name.

	SiO₂	± SD	TiO₂	± SD	Al₂O3	± SD	Fe₂O₃	± SD	MnO	± SD	MgO	± SD	CaO	± SD	Na₂O	± SD	K₂O	± SD	P₂O₅	± SD
Acer saccharum	65.46	1.64	0.36	0.01	5.74	1.27	1.57	0.08	0.28	0.01	2.20	0.07	18.55	0.89	0.94	0.02	3.95	0.09	0.95	0.06
Betula alleghaniensis	47.22	0.57	0.30	0.01	4.76	1.24	1.14	0.09	1.42	0.10	2.38	0.06	39.05	0.36	0.45	0.02	1.88	0.07	1.39	0.12
Betula lenta	68.07	1.39	0.37	0.01	6.75	1.08	2.15	0.09	0.34	0.01	1.77	0.04	17.27	0.50	0.52	0.06	1.94	0.04	0.81	0.03
Fraxinus americana	35.02	1.09	0.24	0.02	4.48	1.49	1.00	0.11	0.10	0.00	3.70	0.20	43.17	1.28	0.85	0.01	7.69	0.62	3.74	0.36
Liriodendron tulipifera	45.38	0.27	0.30	0.01	5.59	1.47	1.30	0.12	0.24	0.01	3.98	0.22	34.04	0.92	0.50	0.04	6.30	0.40	2.36	0.18
Picea abies	79.49	1.53	0.44	0.00	6.52	1.16	1.92	0.11	0.29	0.00	1.25	0.04	7.13	0.26	0.62	0.08	1.74	0.01	0.59	0.03
Pinus resinosa	69.10	0.85	0.43	0.02	7.13	1.03	2.03	0.09	0.72	0.01	2.68	0.03	13.67	0.05	0.69	0.03	2.32	0.04	1.25	0.09
Pinus strobus	65.72	1.37	0.45	0.01	7.28	1.13	2.15	0.10	0.46	0.01	2.52	0.04	15.57	0.62	0.66	0.06	3.20	0.09	1.98	0.07
Populus grandidentata	48.58	0.93	0.28	0.02	5.00	1.20	1.29	0.12	0.80	0.05	5.16	0.22	26.45	0.74	0.46	0.02	8.46	0.32	3.53	0.23
Prunus serontina	73.52	1.42	0.37	0.00	6.00	1.28	1.74	0.10	0.10	0.00	1.85	0.06	12.12	0.22	0.55	0.07	2.56	0.02	1.18	0.07
Quercus alba	28.21	1.91	0.23	0.02	3.94	1.48	0.75	0.09	0.38	0.04	0.86	0.08	60.98	2.87	0.44	0.03	3.82	0.23	0.39	0.04
Quercus montana	59.16	1.21	0.32	0.00	5.19	1.27	1.47	0.09	0.18	0.01	1.60	0.02	27.03	0.36	0.69	0.02	3.58	0.12	0.78	0.04
Quercus rubra	65.76	1.16	0.39	0.01	6.53	0.99	2.07	0.10	0.26	0.01	1.56	0.01	17.40	0.61	0.61	0.06	4.57	0.14	0.84	0.05
Quercus velutina	28.10	2.46	0.24	0.02	4.45	1.58	0.93	0.12	0.35	0.03	3.09	0.20	58.51	3.38	0.44	0.04	2.62	0.15	1.26	0.16
Tsuga canadensis	75.41	1.11	0.41	0.02	6.66	1.04	2.04	0.12	0.57	0.01	1.28	0.03	10.90	0.23	0.57	0.06	1.42	0.05	0.74	0.04
Soil Average (n=16)	81.20	6.57	0.53	0.14	11.35	3.06	3.00	1.07	0.06	0.02	0.79	0.32	0.78	1.47	0.89	0.86	1.29	0.45	0.16	0.09

Table 3. 6 . Mean trace element concentration (in ppm) per species (+ S.E.) and soil average (n=3 readings per element per species). Elements listed in order of increasing atomic weight. Species listed in alphabetical order by Latin name.

	Sc	+ SE	V	+ SE	Cr	+ SE	Co	+ SE	Ni	+ SE	Cu	+ SE	Zn	+ SE	Ga	+ SE	Rb	+ SE	Sr	+ SE
Acer saccharum	2.32	0.27	31.83	0.42	18.04	0.34	4.13	0.04	12.42	0.16	38.46	1.20	184.36	4.02	14.44	0.04	44.52	1.17	495.68	11.17
Betula alleghaniensis	0.70	0.23	17.60	0.09	13.68	0.44	3.45	0.03	6.71	0.34	58.69	0.55	1637.44	7.69	13.96	0.03	33.96	0.21	883.35	6.07
Betula lenta	3.56	0.24	41.25	0.16	26.88	0.49	6.77	0.10	16.14	0.20	36.30	0.64	2232.01	6.58	14.75	0.05	46.10	1.60	453.67	6.57
Fraxinus americana	0.69	0.14	20.61	0.22	17.18	0.32	1.92	0.02	9.55	0.39	351.10	7.07	301.49	2.87	13.46	0.03	39.54	0.16	1269.26	31.11
Liriodendron tulipifera	0.28	0.21	23.15	0.33	14.99	0.55	2.94	0.01	8.41	0.50	89.34	1.00	196.02	2.80	14.30	0.00	37.88	0.35	675.15	11.26
Picea abies	4.70	0.28	46.27	0.55	22.87	0.28	7.59	0.10	18.95	0.24	39.01	0.10	475.09	5.70	14.68	0.05	41.97	0.18	237.90	1.07
Pinus resinosa	3.51	0.18	33.74	0.35	21.95	0.40	7.34	0.10	23.35	0.22	64.21	1.46	539.86	1.51	14.59	0.03	51.15	1.33	268.09	4.28
Pinus strobus	2.57	0.18	30.11	0.47	22.91	0.54	6.18	0.07	24.68	0.09	64.03	0.75	684.77	1.19	14.57	0.05	62.75	0.57	220.35	4.39
Populus grandidentata	0.57	0.20	23.76	0.16	13.94	0.46	7.57	0.06	53.97	0.70	128.50	0.71	3313.72	16.62	14.09	0.04	101.17	1.08	861.66	10.29
Prunus serontina	3.31	0.26	28.67	0.29	19.30	0.71	4.24	0.05	8.43	0.18	50.14	0.34	79.12	0.25	14.28	0.01	45.03	0.24	387.15	1.85
Quercus alba	0.80	0.20	11.58	0.25	6.65	0.71	1.89	0.05	17.99	0.01	53.39	0.36	24.10	0.30	13.01	0.02	46.69	1.09	747.06	8.39
Quercus montana	2.52	0.23	34.80	0.83	16.99	0.56	4.41	0.05	21.00	0.55	57.99	0.68	183.77	1.58	13.96	0.01	48.88	1.13	533.11	4.98
Quercus rubra	3.44	0.27	34.76	0.86	21.77	0.55	5.09	0.01	19.49	0.23	49.52	0.40	80.52	1.96	14.54	0.02	121.24	2.70	284.41	2.31
Quercus velutina	0.86	0.12	17.62	0.09	11.74	0.43	3.11	0.01	12.55	0.39	116.49	4.18	1024.77	4.39	13.68	0.02	45.51	0.71	881.83	16.41
Tsuga canadensis	4.10	0.22	41.16	0.09	23.66	0.40	6.01	0.02	14.69	0.19	60.32	0.11	427.53	3.51	14.65	0.03	35.21	0.60	211.52	4.35
Soil Average (n=16)	6.57	0.49	49.65	4.95	27.99	1.07	7.06	0.64	13.33	0.72	25.88	3.24	70.04	4.41	13.96	0.40	45.17	2.04	41.47	2.06

	Y	+ SE	Zr	+ SE	Nb	+ SE	Cs	+ SE	Ba	+ SE	Hf	+ SE	Ta	+ SE	Pb	+ SE	Th	+ SE	U	+ SE
Acer saccharum	15.81	0.37	158.52	1.60	5.90	0.15	0.81	0.03	551.60	8.35	4.00	0.30	0.41	0.91	11.19	0.04	3.51	0.22	1.03	0.13
Betula alleghaniensis	8.90	0.03	107.63	1.49	4.24	0.06	0.63	0.02	1781.31	31.15	2.52	0.14	0.31	0.88	50.88	0.05	2.37	0.25	0.71	0.10
Betula lenta	16.21	0.14	170.91	2.68	6.39	0.12	1.15	0.01	622.86	4.14	4.32	0.27	0.46	0.90	12.88	0.05	4.49	0.26	1.30	0.08
Fraxinus americana	7.51	0.11	37.57	2.73	2.69	0.10	0.38	0.01	1005.19	14.61	0.70	0.13	0.20	0.92	2.94	0.02	1.50	0.39	0.42	0.08
Liriodendron tulipifera	16.64	0.30	53.02	1.58	3.93	0.09	0.55	0.01	696.85	6.45	1.06	0.08	0.26	0.53	4.60	0.02	2.45	0.28	1.73	0.03
Picea abies	16.01	0.02	317.41	7.49	9.58	0.17	1.10	0.01	900.08	11.05	7.76	0.19	0.61	0.30	34.89	0.07	5.08	0.09	1.54	0.10
Pinus resinosa	14.66	0.11	208.78	3.58	8.29	0.07	1.22	0.04	485.65	6.64	5.24	0.23	0.56	0.54	12.40	0.06	4.77	0.18	1.56	0.13
Pinus strobus	15.56	0.08	97.91	1.10	6.77	0.16	1.29	0.02	316.68	5.84	1.95	0.07	0.51	0.57	30.61	0.03	3.90	0.36	1.36	0.07
Populus grandidentata	26.99	0.25	30.52	0.58	5.36	0.09	0.70	0.01	5279.30	58.99	0.74	0.69	0.35	0.47	3.84	0.03	2.63	0.19	0.83	0.03
Prunus serontina	13.66	0.20	246.62	2.57	6.50	0.02	1.03	0.02	327.22	3.36	6.51	0.03	0.45	0.71	19.70	0.08	4.16	0.10	1.27	0.07
Quercus alba	4.65	0.09	80.49	1.52	2.52	0.11	0.33	0.02	1029.79	10.32	1.88	0.03	0.16	0.90	3.64	0.03	1.09	0.19	0.33	0.13
Quercus montana	11.63	0.07	212.74	4.27	5.13	0.08	0.73	0.03	532.70	8.90	5.71	0.13	0.34	0.80	10.05	0.05	3.68	0.22	1.04	0.10
Quercus rubra	14.34	0.19	201.47	1.09	7.43	0.04	1.43	0.03	382.60	2.98	5.09	0.42	0.54	0.60	4.93	0.08	4.31	0.34	1.19	0.04
Quercus velutina	6.17	0.12	48.20	1.01	2.11	0.04	0.41	0.02	904.60	13.33	1.04	0.10	0.16	0.83	3.66	0.02	1.31	0.27	0.42	0.11
Tsuga canadensis	13.97	0.09	255.31	2.51	8.28	0.04	1.24	0.01	628.48	5.72	6.40	0.03	0.51	0.36	18.80	0.05	4.28	0.22	1.35	0.10
Soil Average (n=16)	20.73	0.84	338.11	14.65	8.95	0.59	1.52	0.07	196.83	8.16	8.31	0.38	0.71	0.02	28.18	3.63	5.88	0.12	1.89	0.04

Table 3. 7 Correlation matrix of (a) trace elements in ash (n=15) and (b) trace elements in soil (n= 16). Spearman's correlation coefficient (ρ) given along with statistical significance. Statistically significant correlations in bold. More statistically significant correlations existed among trace elements in soil (71) than trace elements in wood ash (17).

(a) Trace Element Correlations in Ash

	Sc	V	Cr	Co	Ni	Cu	Zn	Ga	Rb	Sr	Y	Zr	Nb	Cs	Ba	Hf	Ta	Pb	Th	U
Sc	1																			
V	.452	1																		
Cr	.099	.136	1																	
Co	.287	.096	-.152	1																
Ni	-.263	-.012	-.188	-.243	1															
Cu	**-.712****	-.256	-.385	-.317	.240	1														
Zn	-.024	-.369	-.362	.135	**.606**	-.063	1													
Ga	.025	-.246	**-0.544**	**0.575**	-.318	-.018	.376	1												
Rb	.242	.474	.189	.049	-.115	-.252	-.019	-.048	1											
Sr	**-0.638**	-.329	-.370	-.197	.340	**.790****	.264	.192	-.094	1										
Y	.172	.017	.098	.190	-.316	.153	-.034	-.171	.245	.165	1									
Zr	.384	.325	-.368	**0.573**	-.068	-.106	-.154	.130	-.253	-.324	-.462	1								
Nb	.116	.165	-.373	**0.553**	-.178	-.034	.107	**.659****	-.150	.230	-.038	.352	1							
Cs	.200	.488	.034	.133	-.129	-.208	-.261	-.193	.485	-.155	.065	.032	-.120	1						
Ba	-.150	-.322	-.123	-.001	**.614**	-.041	**.870****	.171	-.092	.272	.072	-.264	-.021	-.145	1					
Hf	.495	.511	.052	.067	.097	-.171	-.093	-.275	**-0.522**	-.180	.482	-.364	.135	-.040		1				
Ta	.237	.475	-.047	.149	.155	-.193	.076	-.096	**0.609**	-.063	.025	-.076	-.169	**.771****	.028	.191	1			
Pb	.191	-.021	-.303	.021	-.077	-.143	.182	.329	**-0.547**	-.196	-.343	.246	.386	-.242	.182	.027	-.231	1		
Th	.481	**0.597**	-.473	.414	.006	-.119	.138	.286	.379	-.176	-.205	**0.617**	.374	.248	-.070	.487	.374	.235	1	
U	.476	.246	-.213	-.001	-.011	.036	-.022	.034	.035	.078	**.646****	.180	.272	.091	-.244	.110	.014	-.020	.292	1

(b) Trace Element Correlations in Soil

	Sc	V	Cr	Co	Ni	Cu	Zn	Ga	Rb	Sr	Y	Zr	Nb	Cs	Ba	Hf	Ta	Pb	Th	U
Sc	1																			
V	**.979****	1																		
Cr	-.283	-.396	1																	
Co	**.986****	**.973****	-.319	1																
Ni	**.728****	**.657****	.245	**.702****	1															
Cu	.482	.491	.036	.496	.169	1														
Zn	.368	.312	.098	.400	.451	.389	1													
Ga	**.682****	**.692****	-.382	**.732****	**0.54**	.231	.418	1												
Rb	**.858****	**.807****	-.013	**.886****	**.763****	.459	**0.517**	**.790****	1											
Sr	**.938****	**.965****	**-0.543**	**.954****	.491	**0.516**	.290	**.708****	**.756****	1										
Y	.178	.096	.198	.207	.447	-.241	.329	.475	.407	.030	1									
Zr	-.335	-.406	.406	-.435	.163	**-0.5**	.051	-.269	-.331	**-0.555**	.278	1								
Nb	**.774****	**.694****	.020	**.740****	**.645****	.460	**.642****	**0.594**	**.761****	**.630****	.468	.006	1							
Cs	-.031	-.141	**.691****	-.027	.471	-.229	.226	.159	.384	-.283	**.629****	.332	.204	1						
Ba	**.957****	**.974****	-.481	**.972****	**0.541**	**0.533**	.325	**.725****	**.808****	**.996****	.072	**-0.541**	**.666****	-.204	1					
Hf	-.305	-.396	.440	-.387	.188	-.430	.213	-.194	-.249	**-0.53**	.397	**.970****	.139	.382	**-0.51**	1				
Ta	**.782****	**.693****	.138	**.736****	**.826****	.322	**.644****	**0.577**	**.798****	**0.569**	.496	.167	**.944****	.372	**0.618**	.263	1			
Pb	-.319	-.319	-.292	-.383	-.094	-.168	.160	-.217	-.178	.117	.021	-.217	-.134	-.199	.051	-.328	1			
Th	.338	.237	**0.557**	.319	**0.526**	.449	.344	.373	**0.598**	.159	.328	.068	.488	**0.562**	.225	.134	**0.547**	.166	1	
U	.440	.333	.443	.369	**.811****	-.085	.411	.368	**0.565**	.141	**0.577**	**0.549**	**.640****	**.684****	.203	**0.578**	**.825****	-.266	**0.596**	1

Bold Font and (**) = Correlation is significant at the 0.01 level (2-tailed).
Bold Font = Correlation is significant at the 0.05 level (2-tailed).

Table 3. 8. Mean rare earth concentrations (ppm) of ash per tree species and soil average ± SE. (n=3 readings per element per species). Elements listed in order of increasing atomic weight. Species listed in alphabetical order.

	La	± SE	Ce	± SE	Pr	± SE	Nd	± SE	Sm	± SE	Eu	± SE	Gd	± SE
Acer saccharum	46.99	0.79	30.01	0.93	27.29	0.29	21.81	0.31	14.70	0.55	8.54	0.12	11.23	0.32
Betula alleghaniensis	17.80	0.36	18.76	0.90	14.57	0.35	10.43	0.35	6.79	0.45	4.28	0.16	5.42	0.02
Betula lenta	38.96	0.72	33.11	0.93	25.92	0.35	19.75	0.37	13.38	0.33	7.90	0.08	10.63	0.21
Fraxinus americana	15.50	0.33	14.11	0.94	10.91	0.15	6.79	0.55	4.55	0.35	3.24	0.09	4.83	0.07
Liriodendron tulipifera	45.75	0.21	29.28	0.54	29.79	0.14	23.83	0.39	16.48	0.12	9.45	0.20	12.04	0.22
Picea abies	53.93	0.51	35.01	0.31	27.26	0.48	21.13	0.13	12.95	0.44	7.36	0.09	9.63	0.18
Pinus resinosa	46.83	0.60	35.94	0.55	29.02	0.38	21.93	0.25	12.81	0.55	6.95	0.07	8.95	0.02
Pinus strobus	34.23	0.19	29.63	0.58	23.83	0.17	17.90	0.50	11.75	0.32	6.72	0.20	8.79	0.16
Populus grandidentata	92.39	1.82	30.43	0.48	36.06	0.22	27.40	0.26	16.59	0.14	11.40	0.27	14.47	0.15
Prunus serontina	35.58	0.09	29.49	0.73	23.37	0.52	17.83	0.14	11.39	0.30	6.41	0.11	8.51	0.07
Quercus alba	11.27	0.09	11.50	0.92	8.82	0.20	4.84	0.27	2.64	0.56	2.19	0.07	3.25	0.09
Quercus montana	28.21	0.33	24.33	0.82	20.24	0.31	14.45	0.30	9.49	0.44	5.57	0.21	7.68	0.06
Quercus rubra	45.72	1.11	38.92	0.61	32.56	0.53	25.38	0.48	15.28	0.18	8.18	0.34	9.54	0.07
Quercus velutina	19.59	0.27	15.08	0.85	11.63	0.14	6.93	0.38	4.24	0.48	2.98	0.12	4.35	0.07
Tsuga canadensis	39.96	0.08	32.88	0.37	26.16	0.32	19.17	0.31	12.35	0.43	7.11	0.11	8.75	0.06
Soil Average (n=16)	2.78	0.58	2.44	0.42	1.61	0.35	1.27	0.24	0.96	0.15	0.52	0.09	0.51	0.10

	Tb	± SE	Dy	± SE	Ho	± SE	Er	± SE	Tm	± SE	Yb	± SE	Lu	± SE
Acer saccharum	8.48	0.15	6.85	0.07	5.73	0.16	5.00	0.09	4.85	0.13	4.85	0.04	4.89	0.15
Betula alleghaniensis	4.18	0.21	3.51	0.02	3.29	0.25	3.22	0.07	3.37	0.10	3.49	0.07	3.50	0.06
Betula lenta	8.74	0.09	7.47	0.20	6.55	0.12	5.65	0.01	5.80	0.11	5.43	0.11	5.48	0.06
Fraxinus americana	3.63	0.20	2.77	0.09	2.59	0.14	2.41	0.13	2.45	0.04	2.61	0.09	2.49	0.10
Liriodendron tulipifera	8.88	0.10	6.96	0.16	5.73	0.21	4.85	0.10	4.61	0.13	3.84	0.39	4.01	0.00
Picea abies	7.90	0.12	7.09	0.04	6.43	0.02	5.87	0.14	6.30	0.04	6.26	0.11	6.97	0.04
Pinus resinosa	7.12	0.18	6.42	0.11	5.58	0.14	5.28	0.21	5.49	0.13	5.44	0.10	5.70	0.02
Pinus strobus	7.38	0.10	6.71	0.21	6.16	0.16	5.59	0.11	5.84	0.18	5.96	0.04	5.90	0.16
Populus grandidentata	11.00	0.08	8.51	0.16	6.79	0.22	5.43	0.04	4.70	0.08	4.36	0.06	4.43	0.05
Prunus serontina	7.11	0.01	6.11	0.15	5.50	0.22	5.19	0.10	5.26	0.22	5.29	0.07	5.42	0.18
Quercus alba	2.36	0.19	1.56	0.10	1.54	0.24	1.60	0.08	1.67	0.06	1.75	0.07	1.55	0.04
Quercus montana	6.28	0.17	5.23	0.14	4.60	0.05	4.36	0.13	4.35	0.06	4.34	0.10	4.39	0.05
Quercus rubra	7.72	0.09	6.25	0.04	5.78	0.14	5.23	0.09	5.50	0.07	5.38	0.06	5.44	0.14
Quercus velutina	3.11	0.23	2.18	0.11	2.06	0.20	2.04	0.04	2.13	0.04	2.24	0.08	2.04	0.01
Tsuga canadensis	7.14	0.09	6.25	0.15	5.62	0.15	5.25	0.03	5.49	0.12	5.40	0.07	5.65	0.10
Soil Average (n=16)	0.50	0.07	0.43	0.07	0.39	0.07	0.32	0.05	0.38	0.07	0.32	0.05	0.46	0.08

Table 3. 9. Concentration factor of REE between ash and soil. REEs tended to be 10-15 times more concentrated in ash samples than soils samples. Concentration factor calculated by dividing mean ash concentration per REE (n=15) by mean soil concentration of the same REE (n=16).

	Mean Ash Concentration (ppm)	Mean Soil Concentration (ppm)	Concentration Factor
La	38.18	2.78	14
Ce	27.23	2.44	11
Pr	23.16	1.61	14
Nd	17.30	1.27	14
Sm	11.02	0.96	11
Eu	6.55	0.52	12
Gd	8.54	0.51	17
Tb	6.73	0.50	14
Dy	5.59	0.43	13
Ho	4.93	0.39	13
Er	4.46	0.32	14
Tm	4.52	0.38	12
Yb	4.44	0.32	14
Lu	4.52	0.46	10

Table 3. 10 Correlation matrix of (a) rare earth elements in ash (n=15) and (b) rare earth elements in soil (n= 16). Correlation coefficient (ρ) given along with statically significance statistically significant correlations in bold. All REEs were correlated with one another in both ash and soil.

(a) Rare Earth Element Correlations in Ash													
	La	Ce	Pr	Nd	Sm	Eu	Gd	Td	Dy	Ho	Er	Tm	Yb	Lu
La	1													
Ce	.691**	1												
Pr	.892**	.914**	1											
Nd	.875**	.916**	.997**	1										
Sm	.835**	.895**	.979**	.988**	1									
Eu	.912**	.806**	.964**	.966**	.975**	1								
Gd	.909**	.774**	.939**	.943**	.959**	.993**	1							
Td	.893**	.831**	.952**	.954**	.967**	.985**	.990**	1						
Dy	.847**	.887**	.943**	.946**	.956**	.948**	.953**	.983**	1					
Ho	.794**	.921**	.926**	.930**	.938**	.908**	.907**	.954**	.990**	1				
Er	.720**	.945**	.893**	.898**	.901**	.843**	.837**	.899**	.960**	.987**	1			
Tm	0.605	.948**	.822**	.829**	.829**	.739**	.727**	.805**	.894**	.944**	.982**	1		
Yb	0.537	.914**	.750**	.755**	.746**	.648**	.634*	.725**	.831**	.895**	.950**	.986**	1	
Lu	0.552	.915**	.752**	.758**	.747**	.648**	.635*	.722**	.829**	.891**	.947**	.984**	.995**	1

(b) Rare Earth Element Correlations in Soil													
	La	Ce	Pr	Nd	Sm	Eu	Gd	Td	Dy	Ho	Er	Tm	Yb	Lu
La	1													
Ce	.877**	1												
Pr	.949**	.924**	1											
Nd	.949**	.892**	.934**	1										
Sm	.919**	.924**	.939**	.870**	1									
Eu	.853**	.885**	.883**	.791**	.942**	1								
Gd	.882**	.874**	.924**	.861**	.886**	.935**	1							
Td	.931**	.896**	.917**	.875**	.959**	.959**	.941**	1						
Dy	.814**	.737**	.820**	.760**	.846**	.810**	.791**	.881**	1					
Ho	.910**	.799**	.866**	.864**	.846**	.861**	.916**	.914**	.760**	1				
Er	.788**	.791**	.833**	.774**	.820**	.886**	.890**	.897**	.872**	.846**	1			
Tm	.871**	.844**	.803**	.856**	.794**	.784**	.805**	.877**	.715**	.896**	.785**	1		
Yb	.780**	.741**	.795**	.808**	.764**	.777**	.869**	.839**	.719**	.900**	.846**	.825**	1	
Lu	.871**	.794**	.842**	.775**	.883**	.886**	.845**	.905**	.773**	.939**	.805**	.869**	.804**	1

Bold Font and (**) = Correlation is significant at the 0.01 level (2-tailed).
Bold Font = Correlation is significant at the 0.05 level (2-tailed).

Table 3. 11. Correlation matrix of major oxides against REEs for wood ash samples (n=15). Statistically significant correlation coefficients (ρ) are in bold. SiO_2 and CaO were the only two oxides to have statistically significant correlations with every REE (highlighted in yellow). SiO_2 had statistically significant *positive* relationships with each REE, while CaO had statistically significant *negative* relationship with each REE. (** denotes $p<0.01$ and * denotes $p<0.05$).

	La	Ce	Pr	Nd	Sm	Eu	Gd	Td	Dy	Ho	Er	Tm	Yb	Lu
SiO_2	**.621**[*]	**.860**[**]	**.651**[**]	**.659**[**]	**.653**[**]	**.538**[*]	**.524**[*]	**.620**[*]	**.736**[**]	**.805**[**]	**.882**[**]	**.935**[**]	**.962**[**]	**.965**[**]
TiO_2	.337	**.835**[**]	**.598**[*]	**.604**[*]	**.589**[*]	.452	.427	**.524**[*]	**.661**[**]	**.745**[**]	**.831**[**]	**.911**[**]	**.948**[**]	**.942**[**]
Al_2O_3	.375	**.871**[**]	**.660**[**]	**.663**[**]	**.659**[**]	**.528**[*]	.508	**.597**[*]	**.717**[**]	**.789**[**]	**.854**[**]	**.917**[**]	**.926**[**]	**.909**[**]
Fe_2O_3	.382	**.886**[**]	**.664**[**]	**.663**[**]	**.655**[**]	**.531**[*]	.508	**.609**[*]	**.725**[**]	**.803**[**]	**.868**[**]	**.931**[**]	**.947**[**]	**.926**[**]
MnO	.101	-.053	.011	-.001	-.039	.022	-.019	-.037	-.024	-.040	-.042	-.058	-.046	-.041
MgO	.438	-.103	.220	.209	.215	.353	.378	.290	.186	.089	-.024	-.166	-.241	-.243
CaO	**-.551**[*]	**-.903**[**]	**-.755**[**]	**-.761**[**]	**-.754**[**]	**-.661**[**]	**-.650**[**]	**-.735**[**]	**-.833**[**]	**-.887**[**]	**-.941**[**]	**-.965**[**]	**-.977**[**]	**-.977**[**]
Na_2O	-.027	.159	.077	.100	.127	.059	.088	.099	.136	.150	.177	.193	.254	.239
K_2O	.342	-.185	.149	.141	.142	.274	.288	.202	.064	-.024	-.147	-.287	-.358	-.363
P_2O_5	.279	-.199	.071	.060	.069	.200	.224	.161	.080	.012	-.085	-.200	-.242	-.250
** Correlation is significant at the 0.01 level (2-tailed).														
* Correlation is significant at the 0.05 level (2-tailed).														

4. DISCUSSION

The main goal of this study was to assess the chemistry of wood ash derived from fifteen tree species, compare the ash chemistry to soil chemistry, and interpret interspecific variation among ash samples. Fire temperature reached during the 45 minute controlled burns were significant as these temperatures typically correlate with severe, high intensity, fire events (temperatures above 500°C). Elements or oxides more concentrated in ash than soil samples included MnO, MgO, CaO, K_2O, P_2O_5, Ni, Cu, Zn, Sr, Ba, and all REE's. Of these elements, generally high interspecific variation existed among trees, with *Populus grandidentata* yielding ash with the greatest deviation in elemental concentrations among other tree species.

Lack of statistical differences between top (0-3cm) and bottom (3-7 cm) soil cores seems to convey a chemically homogeneous soil environment immediately after a forest fire (i.e. elements did not have enough time to translocate through the soil profile). Elements still remained in the ash immediately after a fire and will only translocate within soils after leaching starts (i.e., initiated after a rain event). Davis (1959) noted the leaching of minerals from ash does not occur immediately after a fire event. As noted by Darley (2017) Cu and Ba tended to persistent as chemical signatures in soils after a forest fire event. Cu and Ba had higher concentrations in burned soils than in unburned soils. These results from Darley (2017) were likely influenced by Cu and Ba's concentrated nature in ash samples as shown in figure 3.5. Cu and Ba may leach into the soil after a rain event, whereas other elements concentrated in mineral ash may transport out of the burn site and into streams via runoff.

The ability to obtain ICP results on ash chemistry using marine sediment flux

fusion procedures was significant as major concerns existed on the ability to fuse ash

samples with $LiBO_2$ flux due to the differences in densities between the two materials.

Campos *et al.* 2016 digested ash samples in 60% HNO_3 followed by re-digestion with

H_2O_2 and heating for 2 hr 45 min at 95°C, but did not flux fuse the samples at 1050°C.

Unfortunately the flux fusion method used on soils only indicates total availability of

elements whereas the H_2O_2 digestion method would give bioavailable elemental

concentrations. For ash samples, the flux fuse method gives the bioavailable elemental

concentrations because these elements had to be available for trees to sequester from

soils.

4.1 Ash Color

As noted by Ubeda *et al.* (2009) ash color may not necessarily fall within the grey

scale spectrum, but can take on brownish and reddish hues. Bodi *et al.* (2014) conveyed a

reddish hue is likely a result of iron oxidation and other brown hues an indication of other

elements oxidizing. Table 3.2 gives some visual indication that different element maybe

in different proportions among ash samples as all the ash samples have slightly different

hues. Unfortunately, only reporting Munsell colors limits the ability to visually depict

color variation due to its alphanumeric code. Converting Munsell color notation to RGB

values provides a semi-quantitative approach to assessing color variation (on a 0-255 bit

scale) and a method of graphical illustration. Munsell to RGB conversion allows

graphing color on a three dimensional scatter plot with R, G, and B values on each axis

and may facilitate visual grouping of samples based on color (figure 3.1). This

methodology could be useful for future ANOVA analyses on certain elements between ash color groups.

For this research, figure 3.1 shows two distinct clusters of species based on ash color, along the color spectrum of ash. These ash colors (figure 3.1, table 3.2) assert that categorizing ash based on grey scale neglects the possibility of hue variation outside grey scale and, therefore, variation in chemical composition. Fitting a regression plane on the data points helps to convey a mathematical similarity among ash samples based on ash color. Future studies could correlate color to ash chemistry based on the two color groupings. This technique could be a useful field method to rapidly assess ash chemistry based on ash color.

Mathematical limitations noted for the Munsell to RGB conversion existed (MIT, n.d.). Future studies could generate stronger mathematical functions for color conversion or researchers could use colorimeters to directly measure ash color in RGB values. The use of such instruments can also remove researcher subjectivity in color identification. This methodological construct is not much different from a paint color matching software at a hardware/home improvement store. Previous color theory studies have used the Farnsworth-Munsell 100-hue color scale to score and graph color (Lugo & Tiedeman, 1986; Beauchamp *et al.,* 1999); however, direct Munsell to RGB conversion provides a quick and simple way to assess color variation among samples. Munsell colors likely have RGB equivalents (to computer print color charts), but such information would be under copyright by the Munsell Company™.

4.2 Pyrogenic Carbon Content

A considerable amount of carbon remains in charred biomass from all species even after exposure to extreme forest fire temperatures. Both the mixed hardwood and conifer saw dust yielded carbon content of 98-99% carbon (table 3.3), indicating background carbon content in many trees. Therefore, upon complete combustion, wood biomass is reduced to 1-2% of its original mass. Interestingly, the 98-99% reduction in mass was similarly described by Sloane (1954). An approximate wood to ash conversion metric for early US farmers using wood ash as a soil amendment was conveyed as: a half cord of firewood (cord =128 cubic feet volume) would yield enough ash to fill a five gallon bucket (Sloane, 1954). Converting these rough values to the same volumetric units, and a performing a percent loss in mass calculation, resulted in a 98.9% reduction in firewood mass. Thus the remaining 1.1% of material would be mineral ash and supports the LOI results on sawdust samples in this study.

All mean percent pyrogenic carbon values are lower than the sawdust of mixed hardwood and conifer percent carbon content. This was expected as the charred material represents an intermediary product in the production of mineral ash. The lower carbon content in charred samples indicates some organic material has volatized but complete combustion did not occur. *Populus grandidentata* and *Liriodendron tulipifera* had the lowest mean pyrogenic carbon percent and highest remaining mineral percent, meaning these species were the most completely combusted of all the other species. *Populus grandidentata* likely had the greatest combustion completeness as the bark of *Populus* sp. tends to be thin and has little cork surrounding the wood tissue (Davis 1959; DeByle & Winokur, 1985). Davis (1959) further noted *Populus grandidentata* as a species with low

66

fire resistance due to the openness of the tree crown, moderate stand density, and shallow rooting habit. Low wood density likely contributed to the higher combustion completeness as both *Populus grandidentata* and *Liriodendron tulipifera* have the lowest wood densities of all species burned (Alden, 1995).

The significance of charred biomass and its carbon content centers on its persistence in the soil. Charred wood ash serves as a proxy for fire occurrence and climate state of an area on the decadal to millennial time scales (Marlon *et al.,* 2012). On shorter timescales, this material often absorbs plant nutrients and acts as a nutrient source for successive vegetation growth (Marlon *et al.,* 2012). Its dark coloration absorbs solar heat energy, which can modify local ambient soil temperatures after a wildfire on the diurnal timescale (Davis, 1959).

4.3 Major and Trace Elements in Wood Ash

Proportions of major elemental oxides found in this study are similar to the findings of Ohno & Erich (1990) and Bodi *et al*. (2014). Calcium and silica, the two most abundant oxides by percent weight in ash, have a strong negative correlation with one another and considerable variation among tree species. Silica content was greater in soils than ash while calcium content was greater in ash than soils (figure 3.3). A high proportion of silica in ash was expected as the growth medium for trees (soils) had high silica content (81% weight of silica in soils). Calcium was higher in ash because plant biomass requires calcium for growth (Coder 2013). Thus 1% CaO measured in soils and 7 to 60% CaO measured in ash (table 3.5) supports this claim and indicates a biological preference for calcium. Part of the high Ca content in ash might be due to the ashing effect, where removing all the carbon concentrates the remaining mineral material.

67

However it is more likely trees actively sequester calcium from the soils for metabolic and physiologic purposes (table 4.1) (Thomas, 1969; Hanger, 1979; Raven *et al.,* 2002; Coder, 2013).

Both silica and calcium are inorganic components of plant cell walls, but calcium also exists between neighboring cell wall (cross linking pectin chains), used in signal transduction within and between cells, cell division, enzyme activity, and facilitates the proper functioning of guard cell in leaf stomata (Raven *et al.,* 2002; Coder, 2013). Calcium is regarded as a phloem immobile element and only travels via xylem (Lautner & Fromm, 2010). In wood, 90% of all calcium exists as calcium oxalate crystals (CaC_2O_4), with the remaining bound to calmodulin (a protein) or held in cell vacuoles (Coder, 2013). As calcium oxalate, Ca can easily be incorporated into cell walls of wood tissues and immobilized (Lautner & Fromm, 2010; Coder, 2013). Therefore, the amount of cell wall material within wood, and its overall density, is dependent on the physiologic structure of wood tissue (i.e., growth ring habit) (Conners, 2011; Conners, 2015). This likely explains some of the differential abundance in calcium among ashed tree species.

Both hardwood and conifer species were burned and their respective ash analyzed. Conifer species have tracheid cell structures, defined as elongated cells with thin impervious cell walls (Conners, 2015). Conifers can further be grouped as resinous (pitch) or non-resinous (Nelson *et al.,* 2015). Hardwoods contain vessel elements which are tube-like structures (pores in cross section) with thick permeable cell walls. Vessel elements further differentiate hardwoods as ring porous (having different sized pores based on growing season) or diffuse porous (having pores all of the same size) (Conners, 2011). The major difference between tracheid and vessel elements is the thickness of the

cell walls. Tracheids have thinner cell walls, meaning less woody material and an overall lower wood density than species with vessel elements (Conners, 2015). As trees grow, previous tracheid and vessel element growth occupies space further inside their respective tree species, transitioning from the less dense sapwood (active living tissue) to more dense heartwood (passive dead tissue) (Chattaway, 1952).

Thinner cell walls and lower woody material within certain species may explain lower calcium content in certain woods. As seen in figure 3.2, species with tracheids (conifers) generated ash with low calcium content. Species with vessel elements (hardwoods) tended to generate ash with more calcium, possibly due to greater amounts of cell wall material within the wood. Ring porous species (*Quercus spp.* and *F. americana*) generated ash with more calcium than from diffuse porous species (*Acer saccharum, Liriodendron tulipifera,* and *Populus grandidentata*) (figure 3.2). One explanation might be greater amounts of cell wall material existing in ring porous wood tissue, especially in late season growth (Plomion *et al.,* 2001). Diffuse porous species generated ash with calcium contents between conifer species (lowest Ca) and ring porous hardwood species (highest Ca) (figure 3.2). The only major exception to these groupings was ash derived from *Q. rubra,* which had significantly lower calcium content than other ring porous species. Part of this variability might exist since only branches were burned for all species. Branches have cells with less developed cell walls and less organized wood tissue than wood tissue derived from tree trunks (Plomion *et al.,* 2001). Additional studies are needed to see if calcium content differs between dry masses of conifer and hardwood species. This result is similar to Pitman's (2006) discussion on hardwood species having higher calcium and less silica content than conifer tree species.

Other major oxides found concentrated in ash included: MnO, MgO, K_2O, and P_2O_5. Minor elements concentrated in ash included: Ni, Cu, Zn, Sr, and Ba. All of these elements, with the exception of Ba and Sr, are considered essential nutrients for growth (Raven *et al.,* 2002; Coder 2013). Hence, it is expected to find these particular elements concentrated in the wood ash samples. Trees need to actively sequester these elements in various amounts to meet metabolic and physiologic needs. Table 4.1 lists the major metabolic/physiologic functions of these elements for trees, adapted from Coder (2013) and Raven *et al.* (2002).

Most metal elements enter from the soils to the roots in an aqueous solution and are transported from the roots to the branches via xylem channels (Liu *et al.* 2013). Metal transporter molecules like citrate can increase the rate of metal transport in xylem (Coder, 2013). Not considered essential elements for trees, Ba and Sr were significantly concentrated in the ash samples. A similar finding was observed by Darley (2017) which showed ash samples and soil burned soil samples with significantly higher Ba and Sr concentrations than unburned soil samples. Current literature does not explain why ash has high Ba and Sr or why trees would accumulate these elements. One hypothesis is that these elements have similar properties to Ca and Mg (all group 2a alkaline earth metals) and occupy a similar position on the Lyotropic series (Cronan, 2018). Though not as freely exchangeable as Mg and Ca on clay surfaces, Ba and Sr are still exchangeable ions (figure 4.1). They have the ability to break covalent bondage from clay mineral surfaces, suspend in pore water (aqueous form) and pass into root tissues like other metals. Although, Mg and Ca were measured in weight percent but their equivalent concentrations (in ppm) were much greater than the highest Ba or Sr concentrations.

70

Another factor to consider is similar periodic properties among these metal elements. Most major and trace elements significantly enriched in ash all share a similar property: +2 oxidation states. Mg, Ca, Sr, Ba, Ni, Cu, Zn all have +2 oxidation state in the environment. Potassium forms a +1 charge and phosphorus, typically used by plants as orthophosphate, forms a -1 or -2 charge. The presence of Ba and Sr in ash samples might be because of similarities in oxidation state and used as additional electron donors for cellular respiration, photosynthesis, and tissue generation in trees. Current literature does not discuss the usage of Ba and Sr in trees, but further investigations are needed.

4.4 Interspecific Variation of Major and Trace Elements

Fewer significant elemental correlations existed in ash over soil. This qualitative result indicates greater chemical variability in ash over soils (tables 3.4 and 3.7). Elemental variation among species specific ash samples is likely induced by preferential uptake and storage of certain elements by certain tree species. Elemental concentrations above the soil average (figures 3.4 and 3.6) are required by trees for growth, but elemental concentrations below the soil average are likely excluded by the trees. Al_2O3 and Fe_2O_3 have significantly lower percent weights in ash than soil (figure 3.4), an indication of elemental exclusion. Too much of either of these elements can cause toxicity, though iron toxicity rarely occurs in nature (Poschenrieder *et al.*, 2008). Most of the essential trace elements are needed for photosynthesis and plant metabolism, but too much of these micronutrients (e.g., Ni, Cu, Zn) can also cause toxicity.

Many mechanisms exists to prevent such toxicity, but vary among species (Cobbett, 2000; Poschenrieder *et al.*, 2008; Liu *et al.,* 2013). Dominant mechanisms to prevent toxicity include: elemental exclusion by the roots, storage in cell walls, storage in

dead heartwood, storage in leaves as trichomes (modified epidermal cells), or chelation as phytochelatins in cell vacuoles (Cobbett, 2000). Theses mechanisms represent detoxification by compartmentalization to leaves, stems, branches, bark, trunk, or soils (Cobbett, 2000; Coder, 2013). Depending on which "compartment" burns during a fire, or which species utilizes a certain detoxification mechanism, resulting ash chemistry likely varies among species. Exclusion of certain elements by certain species (e.g., *Acer* spp.) will result in overall lower concentrations in ash then metal chelation of the same metal in cell walls by other species.

Silicon likely facilitates metal capture and detoxification through the formation of organo-silicate complexes in cell walls (i.e., silicon forming within polysaccharides, lignin, and proteins) (Currie & Perry, 2007). Organo-silicates alter silicon's traditional +4 valance to that of +5 or +6 (Epstein, 1994; Coder, 2013). This results in hyper-coordination of silicon (Epstein, 1994), which may allow for the formation of organo-silicate metal complexes and provides a mechanism for binding toxic metals in cell walls. In a simplified view, cell walls and/or the heartwood of trees act as repositories for excess nutrients and elements. Binding excessive elements to cell walls, phytochelatins, or in heartwood renders the metal element chemically inert, immobilized, and non-toxic to growth (Cobbett, 2000). Only upon combustion or decomposition can these metals be released from the organic complex back into the soil environment.

Ash derived from *Populus grandidenta, B. lenta* and *B. alleghaniensis* had the greatest concentrations of Ba and Zn, as well as high concentrations of other enriched elements (figure 3.6). Many other works have found high metal concentration (especially Zn) in *Betula* spp. and *Populus* spp. leaf and branch tissue (Brekken & Steinnes, 2004;

Van Nevel *et al.,* 2011; Qian *et al.* 2012). High metal concentrations likely existed in *Populus grandidenta, B.lenta* and *B. alleghaniensis* due to their wide, diffuse, pore spaces in sapwood allowing for high rates of transpiration. Both species are pioneer species and have adapted the ability to rapidly colonize disturbed sites (Molles, 2016). Rapid colonization and transpiration, especially *Populus* spp., means high uptake of water and dissolved metals from soil and into wood tissue. Raven *et al.* (2002) noted that a five year old aspen tree (*Populus* spp.) can move 100 to 200 liters of water per day from the roots to the leaves, more so than any other tree genera. With more dissolved materials flowing through aspens, this may also explain why *Populus grandidenta* had the highest mineral % material after charcoal underwent LOI tests (table 3.3).

4.5 Rare Earth Elements in Wood Ash

REE's seem to behave differently than major and trace elements. All of these elements appeared 10-15 times more concentrated in ash than soils (table 3.9), but do not appear to have significant functions in plant metabolism nor tree growth. The uniform concentration factors likely indicates no preferential uptake of any one REE by trees and might be attributed to the ashing effect discussed in section 4.3. Liberating the organic material concentrates the remaining mineral material. This phenomenon is similarly explained by Peiravi *et al.* (2017). While not studying wood ash, Peiravi *et al.* (2017) noted burning coal concentrates REEs into a potentially economically mineable source of REEs. Coal ash, formed as a byproduct of electricity production, has a globally averaged REE concentration of about 445 ppm (Peiravi *et al.,* 2017), with Zhang *et al.* (2015) reporting REE concentrations as high as 2,000ppm in some regions. LREEs held the greatest percentage of REE content across all coal types, but bituminous coal had the

highest percentage of HREEs (Peiravi *et al.,* 2017). At REE concentrations of 500 to 700 ppm, coal ash could be economically viable source of REEs extraction by sulfuric acid baking/leaching, roast hydrochloric acid leaching, and caustic soda leaching (Peiravi *et al.,* 2017). Since coal and wood are both composed of organic material (and once living plants) the presence of REE's in their respective ashes may not be uncommon. A study by Braithaite *et al.* (2019) also detected significant REE concentrations in leaf ash from various tree species.

In order for REEs to be present in ash, they needed to exist in the soils. However, the source of REEs in soils at SOC is uncertain as the bedrock material is a conglomerate- quartzite-sandstone and not characteristic of REE containing minerals. Typically REEs are found in phosphate minerals of igneous rocks. The presence of REEs, albeit very low in SOC soils (< 5ppm for all REEs), is likely due to the soil's glacial origin. The most recent glaciation event (Wisconsin) derived material from all over North America, including the igneous Canadian Shield (M. Gorring, personal communication). More locally, an igneous body outcrops as the Bemerville intrusion which could be a local source of igneous REE materials for current soil development, but is purely speculative at the moment of this writing. Notably, the nepheline syenite found just a few miles east Sunrise Mountain provides evidence of igneous material transportation via glaciers (Harper, 2013). The agglomeration of glacial materials weathering into soils over time probably represents the source of REE minerals in these soils. A more though investigation is needed. A few of the 270 REE containing minerals are listed in table 4.2 (Ramos *et al*., 2016), but not all – or any – maybe present in soils at SOC.

Presence of REE's in wood ash samples implies trees probably sequestered (not excluded) these element from the soils and translocated them to the branches. REE's do not have a significant influence on plant metabolism nor physiology (Tyler 2008; Ramos *et al.* 2016), which means these elements were likely sequestered "passively" along with other essential elements from the soil matrix. For instance, many REEs are found in phosphatic minerals, such as apatite $[Ca_{10}(PO_4)_6X_2]$ or monazite $[(REE)(PO_4, SiO_4)]$ (Jorjani & Shahbazi, 2016). REE's are also found in carbonates, flourides, and silicates (Tyler, 2004; Ramos *et al.,* 2016). During apatite formation, trivalent REE's can substitute with divalent calcium (Ramos *et al.,* 2016). Upon weathering, apatite dissolves in soil pore water which is then drawn up by the tree roots for its phosphorous content (Tyler, 2004; Ramos *et al.* 2016). Tree uptake of phosphorus/orthophosphates from the soils may also sequester REEs bound to the phosphate anion (Ramos *et al.,* 2016). LREEs are more easily absorbed by plants than HREEs due to the higher mobility of LREEs in soils (Ramos *et al.,* 2016). This statement concurs with the concentrations found in wood ash of this study: all LREE concentrations were greater than HREE concentrations (Figures 3.10 and 3.11).

REE substitution with calcium may explain another mechanisms for REEs movement from soils to biomass. Calcium is drawn into roots by via fine root apoplasts and calcium channels (Lautner & Fromm, 2010), which may also accept REE's of similar ionic radii to Ca. According to Aide &Aide (2012) REEs decrease in ionic radii La to Lu, likely influenced by the behavior of *f* orbital electrons. Once in the tree, the interplays between Ca and REE's in wood tissue may further explain why these elements appear in wood ash. REEs can undergo redistribution via a tree's vascular system, translocating

from the roots to branches and leaves. REEs may eventually replace Ca in cell walls, reversibly bind to carboxylate anions (COOH-) or replace Ca in Ca oxalate crystals in cell vacuoles or cell walls (Faheed *et al.* 2013; Jorjani & Shahbazi, 2016; Ramos *et al.* 2016). Substitution of Ca in cell walls or oxalate crystals prevents any further translocation of the REE's in trees and prevents toxicity (Tyler, 2008; Faheed *et al.* 2013; Ramos *et al.* 2016). One issue with REE-Ca substitution in cell walls is a slight charge imbalance. Ca has a +2 valence and most REEs form a +3 valence, so a slight change the bonding structure during cell wall formation would have to occur. Figure 4.2 shows an idealized Ca organo-silicate complex by Qin *et al.* (2016). Upon burning calcium and/or the REE's would remain in mineral ash as carbon volatizes.

Interspecific variation of the REE ash concentrations are probably linked to biologically mediated processes. *Populus grandidenta* had the highest concentrations of most REEs (figure 3.10 and 3.11) probably because of high transpiration rates (explained in section 4.4). Additionally, *Populus spp.* have a high abundance of arbuscular mycorrhiza hyphae (Neville *et al.,* 2002) which could increase the weathering rate of REE phosphate and carbonate minerals by releasing oxalic acid and chelating compounds into the rhizosphere (Tyler, 2008). Many other tree species studied have fungal hyphae on the roots, but not necessarily in the same proportions as *Populus grandidenta*. Once dissolved, trees may sequester REEs with phosphate, carboxylic, and hydroxide functional groups (Tyler 2008; Ramos *et al.,* 2016), but further investigations are needed. The negative Eu anomaly in ash – but not soil – may be an indication of preferential exclusion of Eu due to difference in valence charge (Eu has a +2 valence while all other

REE's have a +3 valence). Or, Eu may not bind as well to molecules supplying trees with essential nutrients, meaning its uptake by trees would be reduced.

All intercorrelations of REE's in soil and ash are statistically significant (table 3.10a and 3.10b). This is likely due to the similar properties /behaviors among all the REEs and shows no preferential uptake of any one REE by trees. This supports the hypothesis of "passive" uptake of REEs bonded to essential element molecules. However when assessing correlations between REEs and major oxides only calcium and silica have statistically significant correlations for *all* REEs (table 3.11). All the REEs have a positive relationship with silica and negative relationship with calcium (table 3.11). These results likely support hypothesis of organo-silicate complexes forming in cell walls to sequester metals. As silica content increases in wood more REEs may bind with organo-silicates, meaning higher REE concentrations in ash when burned. Similarly, a negative correlation of REEs with calcium supports the hypothesis of REE substitution with calcium. As more REEs are sequestered by trees (likely though bio-augmentation of soils and bio-chemical weathering of REE containing minerals) they replace Ca in cell walls and in calcium oxalate crystals. This replacement leads to a slightly lower overall Ca content. Greater replacement of Ca by REEs could justify lower Ca content in ash, both of which are likely influenced by the physiologic structure of wood tissue (discussed in section 4.3).

Figure 4.1. Lyotropic series of exchangeable cation adsorption to clay minerals based on cation charge density. This preferential series shows the range of weakly boundg cations (Li^+) to strongly bound cations (Al^{3+}) on clay particles. Sr and Ba hold similar charge densities and similar position in the sequence, but have a slightly greater binding affinity to clay particles than Mg and Ca. Adapted from Cronan (2018).
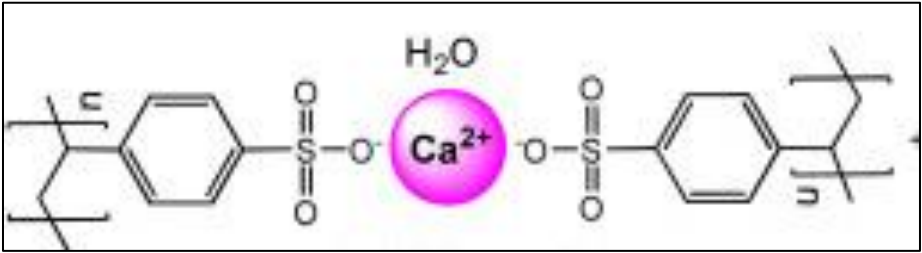

Figure 4. 2. Idealized bonding structure of an organo-silicate with calcium. Replacement of calcium by an REE would leave a change imbalance during cell wall formation, likely inducing a slightly different bonding structure in the cell wall. Figure adapted from Qin *et al.* (2016).

Table 4.1. Essential elements for tree growth. Elements listed in alphabetical order. Adapted from Raven *et al.* (2002) and Coder (2013).

Element	Function in Trees
Calcium (Ca)	Mainly exists as calcium oxalate; incorporated during cell wall formation; crosslinks pectin chains between cell walls; facilitates signal transduction in cell, cell division and is an enzyme activator.
Copper (Cu)	Found as phytochelatins and ketocarboxylatocopper(II) complexes.An enzyme activator, source of electrons for electron transport in respiration and photosynthesis. It forms plastocynin (copper containing protein) and decomposes free radical oxygen in cells.
Magnesium (Mg)	Exists as Mg^{2+}, highly mobile. Needed to form chlorophyll molecules in leaves, an enzyme activator, stabilizes nucleic acids, activates proton pumps in membranes, needed in electron transport.
Manganese (Mn)	Enzyme activator, decomposes free radical oxygen in tissue, stimulates lignification and other plant defensive compounds.
Nickel (Ni)	Enzyme activator for unease (converting urea to CO_2 and ammonia). Increases disease resistance.
Phosphorous (P)	Forms phospholipids, necessary for ADP and ATP energy molecules, DNA and RNA formation, acts as a pH buffer within cells.
Potassium (K)	Exists as K^+. Needed for sodium potassium pump functioning; operates stomata to maintain electronic and moisture equilibrium. Facilitates protein synthesis; activates organic molecules creation.
Silicon (Si)	Exits as Si^{5+} or Si^{6+}. Structural support, stimulates phytoalexins (plant defensive compounds), stiffens cell walls, manages metal toxicity (forming metal complexes)
Zinc (Zn)	Found only in divalent (2+) form. An enzyme activator. Facilitates transcription of DNA, gene expression and the synthesis of auxin (growth hormone).

Table 4.2 Mineral that commonly have REE substitution. Adapted from Aide and Aide (2012).

Mineral	Formula	Substitutions
Allanite	$(Ce, Ca, Y)_2(Al, Fe^{2+}, Fe^{3+})_3(SO_4)_3OH$	REE replace Ca
Sphene	$CaTiSiO^5$	REE replace Ca
Zircon	$ZrSiO_4$	HREE replace Zr
Apatite	$A_5(XO_4)_3(F, OH, Cl)$; A = Ca or REE	REE replace Ca
Monazite	$(REE)PO_4$	
Xenotime	YPO_4	REE replaces Y
Rhabdophane	$(Ce, La)PO4$	REE replaces La
Bastnaesite	La(REE)-fluorocarbonate	

5. CONCLUSION

The overall results show the complexity of biogeochemical cycling within the forest fire environment. Ash is an interdisciplinary medium, influenced by biological, ecological, chemical, pedological, hydrological, climatological, and geological factors. A proper analysis of ash in the soil environment not only recognizes the specific biological mechanisms accounting for interspecific variation but also integrates the broader environmental context of material generation. Fire merely expedites one segment of the material cycle, causing a sudden influx of material into soil which re-equilibrates over short and long time scales. Elemental cycling by ordinary biological decomposition occurs over longer periods of time. Hence, an influx of nutrients after one fire event can be equivalent to a centuries worth of biological decomposition (Bodi *et al.,* 2014).

Agricultural applications over-generalize wood ash as a source of calcium and potash (Slone, 1956; Gliessman, 2015), but neglect the wide array of other available elements at various concentrations presented here. Ash not only influences soil chemistry after a fire, but is influenced by the elemental uptake by its parent material (wood tissue). The chemistry of wood tissue is further influenced by biological, geological, and pedological factors during growth. Therefore, the pre-fire tree assemblage has the greatest control over post-fire ash chemistry on the micro scale. Some tree species may have preferential affinity, exclusivity, or differing detoxification mechanisms for excess elemental uptake, which explains elemental variability among species specific ashes. High certainty exists that many elements found more concentrated in ash than soil (MnO, MgO, CaO, K_2O, P_2O_5, Ni, Cu, Zn) were a result of the need for these elements in plant metabolic and physiologic functions. Other concentrated elements, such as Sr, Ba, and all

REEs, might be a result of passive sequestration by trees, taken up along with essential elements due to similar periodic properties or similar ionic radii.

From a forestry management perspective, fire not only rapidly (and economically) removes excessive woody material (Davis 1959), but also facilitates an influx of elements useful for forest re-growth (Ubeda *et al*., 2009). This study highlights concentrated elements in ash and proposes possible mechanisms for pyrogenic elemental cycling from soil to trees to ash and back to soils. Burning biomass concentrates many essential elements for post-fire forest recovery. Conversely, harvesting biomass for timber and fuel removes these essential elements from the forest system and prevents recycling back to the soils. Pitman (2006) argued for the use of biofuel ash in forest systems to replace essential elements lost from logging. However, based on this study, it could be argued that fertilizing forest ecosystems with wood ash needs to match species specific ash types to the desired forest assemblage. Due to seemingly high interspecific variability in ash composition, biofuel ash derived from mixed oak forest materials should be applied to logged mixed oak forests while biofuel generated from coniferous forest materials should be applied to logged coniferous forests.

Many early forestry works have painted fire as an "enemy of forests" (Davis 1959; Allen & Sharpe, 1960), with strong fire suppression policies swaying a negative public stigma on fire in the forest. However, more recent fire policy has shifted towards contolled burnings to reduce fuel hazards (Hutto *et al.,* 2016). Low intensity controlled fire events can provide much needed fuel load reduction, stimulate successive tree growth, reduce invasive species colonization, eradicate disease, propagate desired timer species, and above all: maintain a healthy mixed successional forest mosaic.

Finally, this study supports results by Darley (2017) in regards to chemical signatures in burned soils. It validates Darley (2017) hypothesis that Cu, Ba, Sr, MnO, and CaO signatures found in burned soils stem from the mineral ash influx to the soil matrix. Further studies need to assess the mobility of these elements post-fire though the pedosphere (migration in the soil profile), hydrosphere (transportation of ash material to streams and wetlands with runoff), and the ecosphere (elemental sequestration by pioneer herbaceous and tree species). The culmination of these studies can unlock a better understanding of the effects of rapid material transformation in a forest system and how the biogeochemical cycle re-equilibrates after a significant environmental perturbation. This research solves the missing link between the vegetative component of ash generation and the pyrogenic chemical signatures found in burned soils.

6. REFERENCES

Ågren, G. I., & Weih, M. (2012). Plant stoichiometry at different scales: element concentration patterns reflect environment more than genotype. *New Phytologist*, *194*(4), 944-952.

Aide, M. T., & Aide, C. (2012). Rare earth elements: their importance in understanding soil genesis. *ISRN Soil Science*, *2012*.

Alden, H.A. (1995). Hardwoods of North America. Gen. Tech. Rep. FPL–GTR–83. Madison, WI: U.S. Department of Agriculture, Forest Service, Forest Products Laboratory.

Allen, S.W., & Sharpe, G.W. (1960) *An Introduction to American Forestry.* 3rd edition. New York, NY: McGraw-Hill Book Company.

Arthur, M. A., Blankenship, B. A., Schörgendorfer, A., Loftis, D. L., & Alexander, H. D. (2015). Changes in stand structure and tree vigor with repeated prescribed fire in an Appalachian hardwood forest. *Forest Ecology and Management*, *340*, 46-61.

Augusto, L., Bakker, M. R., & Meredieu, C. (2008). Wood ash applications to temperate forest ecosystems—potential benefits and drawbacks. *Plant and Soil*, *306*(1-2), 181-198.

Beauchamp, M. S., Haxby, J. V., Jennings, J. E., & DeYoe, E. A. (1999). An fMRI version of the Farnsworth–Munsell 100-Hue test reveals multiple color-selective areas in human ventral occipitotemporal cortex. *Cerebral Cortex*, *9*(3), 257-263.

Ben-Dor, E., & Banin, A. (1989). Determination of organic matter content in arid-zone soils using a simple "loss-on-ignition" method. *Communications in Soil Science and Plant Analysis*, *20*(15-16), 1675-1695.

Bird, M. I., Wynn, J. G., Saiz, G., Wurster, C. M., & McBeath, A. (2015). The pyrogenic carbon cycle. *Annual Review of Earth and Planetary Sciences*, *43*, 273-298.

Blackwelder, E. (1933). The insolation hyphothesis of rock weathering. *American Journal of Science*, (152), 97-113.

Bodí, M. B., Martin, D. A., Balfour, V. N., Santín, C., Doerr, S. H., Pereira, P., & Mataix-Solera, J. (2014). Wildland fire ash: production, composition and eco-hydro-geomorphic effects. *Earth-Science Reviews*, *130*, 103-127.

Bodí, M. B., Mataix-Solera, J., Doerr, S. H., & Cerdà, A. (2011). The wettability of ash from burned vegetation and its relationship to Mediterranean plant species type, burn severity and total organic carbon content. *Geoderma*, *160*(3-4), 599-607.

Bond, W. J., & Keeley, J. E. (2005). Fire as a global 'herbivore': the ecology and evolution of flammable ecosystems. *Trends in ecology & evolution*, *20*(7), 387-394.

Braithaite B.R. & Richardson, J.B. (2019) Retention of trace metals in urban forests and soils near municipal waste incineration facilities in northeastern U.S. In Northeastern Geological Society of America Annual Meeting. Portland, ME: Geological Society of America, Northeastern chapter.

Brachfeld & Gorring (n.d.) Marine Sediment ICP sample preparation procedures. Montclair State University, Montclair NJ.

Brekken, A., & Steinnes, E. (2004). Seasonal concentrations of cadmium and zinc in native pasture plants: consequences for grazing animals. *Science of the Total Environment*, *326*(1-3), 181-195.

Burton, C. A., Hoefen, T. M., Plumlee, G. S., Baumberger, K. L., Backlin, A. R., Gallegos, E., & Fisher, R. N. (2016). Trace Elements in Stormflow, Ash, and Burned Soil following the 2009 Station Fire in Southern California. *PloS One*, 11(5), e0153372. https://doi.org/10.1371/journal.pone.0153372.

Caldwell, T. G., Johnson, D. W., Miller, W. W., & Qualls, R. G. (2002). Forest floor carbon and nitrogen losses due to prescription fire. *Soil Science Society of America Journal*, *66*(1), 262-267.

Callanan, J., Espinal, K., Grune, D., Lach, M., Pope, G., Hazen, M., & DaSilva, M. (2017). Impacts to Surface Soil as a Result of the 16 Mile Fire, Cresco PA, USA. In American Association of Geographers Annual Meeting. Boston: American Association of Geographers.

Campos, I., Vale, C., Abrantes, N., Keizer, J. J., & Pereira, P. (2015). Effects of wildfire on mercury mobilisation in eucalypt and pine forests. *Catena*, *131*, 149-159.

Certini, G. (2005). Effects of fire on properties of forest soils: a review. *Oecologia*, *143*(1), 1-10.

Certini, G. (2013). Fire as a soil-forming factor. *Ambio*, *43*(2), 191-195.

Chattaway, M. M. (1952). The sapwood-heartwood transition. *Australian Forestry*, *16*(1), 25-34.

Cheatham M. M., Sangrey W. F., and White W. M. (1993) Sources of error in external calibration ICP-MS analysis of geological samples and an improved non-linear drift correction procedure. Spectrochimica Acta 48b, E487–E506.

Cobbett, C. S. (2000). Phytochelatins and their roles in heavy metal detoxification. *Plant physiology*, *123*(3), 825-832.

Conners, T. (2011). The basics of wood identification. *Kentucky Woodlands Magazine*, *6*(1), 4-6.

Conners, T. (2015). Distinguishing Softwoods from Hardwoods. Retrieved from https://uknowledge.uky.edu/cgi/viewcontent.cgi?article=1106&context=anr_reports

Coder, Kim D. 2013. Essential Elements of Tree Health. University of Georgia Warnell School of Forestry & Natural Resources Monograph WSFNR13-6.

Cohn, J. S., Di Stefano, J., Christie, F., Cheers, G., & York, A. (2015). How do heterogeneity in vegetation types and post-fire age-classes contribute to plant diversity at the landscape scale?. *Forest Ecology and Management*, *346*, 22-30.

Collins, B. R., & Anderson, K. H. (1994). *Plant Communities of New Jersey*. New Brunswick, NJ: Rutgers University Press. Print.

Cronan, C. S. (2018). Soil biogeochemistry. In *Ecosystem Biogeochemistry* (pp. 11-29). Springer, Cham.

Currie, H. A., & Perry, C. C. (2007). Silica in plants: biological, biochemical and chemical studies. *Annals of Botany*, *100*(7), 1383-1389.

Darley, J.S. (2017) Watershed Sub-Basin Scale Forest Fire Impacts on Soil Chemistry: A Case Study in Delaware State Forest, Pennsylvania, USA. *Theses, Dissertations and Culminating Projects*. 10. https://digitalcommons.montclair.edu/etd/10

Davis, K.P. (1959) *Forest Fire: Control and Use.* New York: NY: McGraw-Hill Book Company.

DeBano, L. F., Neary, D. G., & Folliott, P. F. (1998). *Fire effects on ecosystems*. John Wiley & Sons.

DeBano, L. F. (2000). The role of fire and soil heating on water repellency in wildland environments: a review. *Journal of Hydrology*, *231*, 195-206.

DeByle, N. V., & Winokur, R. P. (1985). Aspen: ecology and management in the western United States.

Demeyer, A., Nkana, J. V., & Verloo, M. G. (2001). Characteristics of wood ash and influence on soil properties and nutrient uptake: an overview. *Bioresource technology*, *77*(3), 287-295.

Epstein, E. (1994). The anomaly of silicon in plant biology. *Proceedings of the National Academy of Sciences*, *91*(1), 11-17.

Etiegni, L., & Campbell, A. G. (1991). Physical and chemical characteristics of wood ash. *Bioresource technology*, *37*(2), 173-178.

Evans, A. M., & Perschel, R. (2009). A review of forestry mitigation and adaptation strategies in the Northeast US. *Climatic Change*, *96*(1-2), 167-183.

Faheed, F., Mazen, A., & Elmohsen, S. A. (2013). Physiological and ultrastructural studies on calcium oxalate crystal formation in some plants. *Turkish Journal of Botany*, *37*(1), 139-152.

Flannigan, M. D., Stocks, B. J., & Wotton, B. M. (2000). Climate change and forest fires. *Science of the total environment*, *262*(3), 221-229.

Foster, D. R., & Orwig, D. A. (2006). Preemptive salvage harvesting of New England forests: When doing nothing is a viable alternative. *Conservation Biology, 20* (4), 959-970.

Glaser, B., Haumaier, L., Guggenberger, G., & Zech, W. (2001). The'Terra Preta'phenomenon: a model for sustainable agriculture in the humid tropics. *Naturwissenschaften*, *88*(1), 37-41.

Gliessman, S.R. (2015). *Agroecology: The Ecology of Sustainable Food Systems*, 3rd ed. Bosa Roca: CRC Press.

Goforth, B. R., Graham, R. C., Hubbert, K. R., Zanner, C. W., & Minnich, R. A. (2005). Spatial distribution and properties of ash and thermally altered soils after high-severity forest fire, southern California. *International Journal of Wildland Fire*, *14*(4), 343-354.

Govindaraju, K. (1989). 1989 compilation of working values and sample description for 272 geostandards. *Geostandards Newsletter*, *13*, 1-113.

Govindaraju, K. (1994). 1994 compilation of working values and sample description for 383 geostandards. *Geostandards newsletter*, *18*, 1-158.

Hanger, B. C. (1979). The movement of calcium in plants. *Communications in Soil Science and Plant Analysis*, *10*(1-2), 171-193.

Harper (2013) *Roadside Geology of New Jersey*. Missoula, MT: Mountain Press.

Hicke, J. A., Meddens, A. J., & Kolden, C. A. (2016). Recent tree mortality in the western United States from bark beetles and forest fires. *Forest Science*, *62*(2), 141-153.

Hutto, R. L., Keane, R. E., Sherriff, R. L., Rota, C. T., Eby, L. A., & Saab, V. A. (2016). Toward a more ecologically informed view of severe forest fires. *Ecosphere*, *7*(2), e01255.

Jorjani, E., & Shahbazi, M. (2016). The production of rare earth elements group via tributyl phosphate extraction and precipitation stripping using oxalic acid. *Arabian journal of chemistry*, *9*, S1532-S1539.

Keeley, J. E., Pausas, J. G., Rundel, P. W., Bond, W. J., & Bradstock, R. A. (2011). Fire as an evolutionary pressure shaping plant traits. *Trends in plant science*, *16*(8), 406-411.

Kloprogge, J. T., Boström, T. E., & Weier, M. L. (2004). In situ observation of the thermal decomposition of weddelite by heating stage environmental scanning electron microscopy. *American Mineralogist*, *89*(1), 245-248.

Kodas, M. (2012). A growing fire threat in the eastern U.S. *Natural Resources Defense Council.* Retried 29 May 2018 from: https://thinkprogress.org/a-growing-fire-threat-in-the-eastern-u-s-c9651be2a96d/

Kumar, T., & Verma, K. (2010). A Theory Based on Conversion of RGB image to Gray image. *International Journal of Computer Applications*, *7*(2), 7-10.

Lautner, S., & Fromm, J. (2010). Calcium-dependent physiological processes in trees. *Plant Biology*, *12*(2), 268-274.

Leite, V, *et al* (2018) Group 2: NJSOC Leach field soil pit. Soil survey conducted for 2018 Field Geology Course. M Gorring, G. Pope, J Galster, instructors, Montclair State University. Sandyston, NJ.

Liodakis, S., Katsigiannis, G., & Kakali, G. (2005). Ash properties of some dominant Greek forest species. *Thermochimica Acta*, *437*(1-2), 158-167.

Liu, W. T., Ni, J. C., & Zhou, Q. X. (2013). Uptake of heavy metals by trees: prospects for phytoremediation. In *Materials Science Forum* (Vol. 743, pp. 768-781). Trans Tech Publications.

Lugo, M., & Tiedeman, J. S. (1986). Computerized scoring and graphing of the Farnsworth-Munsell 100-hue color vision test. *American journal of ophthalmology*, *101*(4), 469-474.

Marlon, J. R., Bartlein, P. J., Gavin, D. G., Long, C. J., Anderson, R. S., Briles, C. E., & Scharf, E. A. (2012). Long-term perspective on wildfires in the western USA. *Proceedings of the National Academy of Sciences*, *109*(9), E535-E543.

Masuda A., Nakamura N., and Tanaka T. (1973). Fine structure of mutually normalized rare-earth patterns of chondrites. *Geochimica et Cosmochimica Acta* (37) 239-248.

MIT (n.d.). Munsell Color Pallet. Retrieved from http://pteromys.melonisland.net/munsell/

Molles, M.C. (2016). *Ecology: Concepts and applications*, 8th ed. New York: McGraw-Hill.

Munsell Color. (2010). *Munsell soil color charts : with genuine Munsell color chips.* Grand Rapids, MI :Munsell Color.

Nelson, G., Earle, C., Spellenberg, R. (2014) *Trees of Eastern North America.* Princeton, NJ: Princeton University Press.

Neville, J., Tessier, J. L., Morrison, I., Scarratt, J., Canning, B., & Klironomos, J. N. (2002). Soil depth distribution of ecto-and arbuscular mycorrhizal fungi associated with *Populus tremuloides* within a 3-year-old boreal forest clear-cut. *Applied Soil Ecology*, *19*(3), 209-216.

NJDEP (2014). Wildfire Hazard Mitigation. New Jersey Forest Fire service. Retrieved 20 April 2019 from https://www.state.nj.us/dep/parksandforests/fire/wildfire_hazard_mitigation.htm

NRCS (2019). Web Soil Survey of New Jersey School of Conservation. *Natural Resource Conservation Service.* Retrieved from https://websoilsurvey.sc.egov.usda.gov/App/HomePage.htm

Ohno, T., & Erich, M. S. (1990). Effect of wood ash application on soil pH and soil test nutrient levels. *Agriculture, ecosystems & environment*, *32*(3-4), 223-239.

Peiravi, M., Ackah, L., Guru, R., Mohanty, M., Liu, J., Xu, B., & Chen, L. (2017). Chemical extraction of rare earth elements from coal ash. *Minerals & Metallurgical Processing*, *34*(4), 170-177.

Pereira, P., Úbeda, X., & Martin, D. A. (2012). Fire severity effects on ash chemical composition and water-extractable elements. *Geoderma*, *191*, 105-114.

Petrova, S., Yurukova, L., & Velcheva, I. (2014). Possibilities of using deciduous tree species in trace element biomonitoring in an urban area (Plovdiv, Bulgaria). *Atmospheric Pollution Research*, *5*(2), 196-202.

Pitman, R. M. (2006). Wood ash use in forestry–a review of the environmental impacts. *Forestry: An International Journal of Forest Research*, *79*(5), 563-588.

Plomion, C., Leprovost, G., & Stokes, A. (2001). Wood formation in trees. *Plant physiology*, *127*(4), 1513-1523.

Pope, G., Callanan, J., & Gorring, M. (2012). A reassessment of soil chemistry and pedogenesis following intense forest fires. In 2012 Annual Meeting, Middle States Division of the Association of American Geographers. Shippensburg, Pennsylvania.

Poschenrieder, C., Gunsé, B., Corrales, I., & Barceló, J. (2008). A glance into aluminum toxicity and resistance in plants. *Science of the total environment*, *400*(1-3), 356-368.

Qian, Y., Gallagher, F. J., Feng, H., & Wu, M. (2012). A geochemical study of toxic metal translocation in an urban brownfield wetland. *Environmental pollution*, *166*, 23-30.

Qin, Z., Ren, X., Shan, L., Guo, H., Geng, C., Zhang, G., & Liang, Y. (2016). Nacrelike-structured multilayered polyelectrolyte/calcium carbonate nanocomposite membrane via Ca-incorporated layer-by-layer-assembly and CO2-induced biomineralization. *Journal of Membrane Science*, *498*, 180-191.

Radeloff, V. C., Hammer, R. B., Stewart, S. I., Fried, J. S., Holcomb, S. S., & McKeefry, J. F. (2005). The wildland–urban interface in the United States. *Ecological applications*, *15*(3), 799-805.

Ramos, S. J., Dinali, G. S., Oliveira, C., Martins, G. C., Moreira, C. G., Siqueira, J. O., & Guilherme, L. R. (2016). Rare earth elements in the soil environment. *Current Pollution Reports*, *2*(1), 28-50.

Reynard-Callanan, J. R., Pope, G. A., Gorring, M. L., & Feng, H. (2010). Effects of high-intensity forest fires on soil clay mineralogy. *Physical Geography*, *31*(5), 407-422.

Raven, P.H., Johnson, G.B., Losos, J.B., Singer, S.R. (2002). *Biology* 7th edition. New York: McGraw Hill.

Roy, David P., et al. "Field estimation of ash and char colour-lightness using a standard grey scale." *International Journal of Wildland Fire* 19.6 (2010): 698-704.

Santín, C., & Doerr, S. H. (2016). Fire effects on soils: the human dimension. *Phil. Trans. R. Soc. B*, *371*(1696), 20150171.

Schaetzl, R.J. & Thompson, M.L. (2015). *Soils: Genesis and Geomorphology*, 2nd ed. New York, New York: Cambridge University Press.

Sloane, E. (1956). *Eric Sloane's America.* New York, NY: Amaranth Press.

Smith, J. E., Kluber, L. A., Jennings, T. N., McKay, D., Brenner, G., & Sulzman, E. W. (2017). Does the presence of large down wood at the time of a forest fire impact soil recovery?. *Forest Ecology and Management*, *391*, 52-62.

St. Clair, S. B., & Lynch, J. P. (2005). Element accumulation patterns of deciduous and evergreen tree seedlings on acid soils: implications for sensitivity to manganese toxicity. *Tree Physiology*, *25*(1), 85-92.

Stephens, S. L., & Ruth, L. W. (2005). Federal forest-fire policy in the United States. *Ecological applications*, *15*(2), 532-542.

Stokes, M., Anderson, M., Chandrasekar, S., Motta, R. (1996) *A Standard Default Color Space for the Internet – sRGB.* Version 1.10.

Thiffault, E., Hannam, K. D., Quideau, S. A., Paré, D., Bélanger, N., Oh, S. W., & Munson, A. D. (2008). Chemical composition of forest floor and consequences for nutrient availability after wildfire and harvesting in the boreal forest. *Plant and Soil*, *308*(1-2), 37-53.

Thomas, W. A. (1969). Accumulation and cycling of calcium by dogwood trees. *Ecological Monographs*, *39*(2), 101-120.

Thomas,D., Butry, D., Gilbert, S., Webb, D., Fung, J. (2017) The Costs and Losses of Wildfires A Literature Review. *NIST Special Publication 1215*. https://doi.org/10.6028/NIST.SP.1215

Tyler, G. (2004). Rare earth elements in soil and plant systems-A review. *Plant and soil*, *267*(1-2), 191-206.

Úbeda, X., Pereira, P., Outeiro, L., & Martin, D. A. (2009). Effects of fire temperature on the physical and chemical characteristics of the ash from two plots of cork oak (Quercus suber). *Land degradation & development*, *20*(6), 589-608.

Ulery, A. L., Graham, R. C., & Bowen, L. H. (1996). Forest fire effects on soil phyllosilicates in California. *Soil Science Society of America Journal*, *60*(1), 309-315.

Van Nevel, L., Mertens, J., Staelens, J., De Schrijver, A., Tack, F. M., De Neve, S., & Verheyen, K. (2011). Elevated Cd and Zn uptake by aspen limits the phytostabilization potential compared to five other tree species. *Ecological Engineering*, *37*(7), 1072-1080.

Verma, S., & Jayakumar, S. (2012). Impact of forest fire on physical, chemical and biological properties of soil: A review. *Proceedings of the International Academy of Ecology and Environmental Sciences*, *2*(3), 168 – 176.

Westerling, A. L., Hidalgo, H. G., Cayan, D.R., Swetnam, T.W. (2006). Warming and earlier spring increase western U.S. forest wildfire activity. *Science 313* (5789), 940-943.

Witte, R. W., & Epstein, J. B. (2005). Surficial Geologic Map of the Culvers Gap Quadrangle, Sussex County, New Jersey. *New Jersey Geological Survey, Survey, New Jersey Geological*.

Witte, R. W. (2008). Surficial geological map of the Branchville quadrangle, Sussex County, New Jersey.

Zhang, W., Groppo, J., & Honaker, R. (2015). Ash beneficiation for REE recovery. In *2015 World of Coal Ash (WOCA) Conference* (pp. 1-11).